Title
Selecting Between One-Dimensional and Two-Dimensional Hydrodynamic Models for Ecohydraulic Analysis

Authors
Gibson, Stanford A
Pasternack, Gregory B

Publication Date
2015

DOI
10.1002/rra.2972

Peer reviewed

Selecting Between One- and Two-Dimensional Hydrodynamic Models for Ecohydraulic Analysis

S.A. Gibson[a] and G.B. Pasternack[b]

[a]Hydrologic Engineering Center, Davis, CA 95616, USA.

[b]Department of Land, Air, and Water Resources, University of California at Davis, Davis, CA 95616-8628, USA

Abstract

Aquatic habitat assessment and river restoration design require geospatially explicit maps of hydraulic conditions. Diverse mechanistic ecohydraulic models compute spatially explicit depth and velocity results to evaluate habitat suitability spatially as a function of these abiotic conditions. This study compared depth and velocity results from two-dimensional (2D) and one-dimensional (1D) hydraulic models with algorithms that laterally discretize 1D velocity and interpolate depth and velocity spatially based on the Laplacian heat mapping approach. These ‘conveyance distributed’ methods constitute ‘best 1D modeling practice’, and were compared to 2D results for the first time. The 1D and 2D models were applied to three morphologically distinct reaches (leveed, meandering, and anastomosing) for three flows (base, bankfull, and flood flows) of the partially regulated, gravel/cobble lower Yuba River in north-central California. The test metrics were the coefficient of determination (R^2) and the median absolute residual ($|\tilde{\square}|$). These metrics quantified the incremental uncertainty 1D approximation incurs, results which make explicit cost-benefit processes of model selection possible. Finally, velocity residual maps were analyzed to identify regions and processes where residuals were high, indicating divergence from the 1D assumptions. Paired data (1D-2D) fell between $0.94 \geq R^2 \geq 1.00$ ($R^2_{mean}=0.98$ and $R^2_{median}=0.99$) for depth and median absolute residuals were all $3.8 \leq |\tilde{\square}| \leq 7.2\%$ (i.e. 50% of residuals are approximately within ±1.7 to 3.6%). Higher flows and lower gradient reaches had lower residuals and higher R^2. Velocity diverged more, particularly for base flow in anastomosing reaches ($0.42<R^2<0.58$). One-dimensional, conveyance distributed, assumptions performed better for other channel types, where $0.69 < R^2 < 0.81$ ($R^2_{mean}=0.75$ and $R^2_{median}=0.77$), with median absolute residuals between $9.6\% > |\tilde{\square}| > 22.4\%$ (i.e. ~±4.6 to ±11.2%), where $|\tilde{\square}|_{mean}=14.2\%$ and $|\tilde{\square}|_{median}=13\%$ (~±7.1 and 6.5%). The conveyance distributed 1D velocity model performed best where the orthogonal flow assumptions obtained and where side channels did not transition from backwater to conveying area between flows.

Keywords: hydraulic modeling, river modeling, ecohydraulics, ecohydraulic modeling, gravel-bed rivers

1 Introduction

Many riverine habitat studies and projects require ecohydraulic modeling (Mouton et al., 2007; Wu and Mao, 2007; Hauer et al., 2011; Maddock et al., 2013). Prescribed flows and restoration designs are often based on and evaluated with these models (Elkins et al., 2007; Papanicolaou et al., 2011). Models can yield detailed spatial patterns at "near-census" resolution of ~ 1 m over tens of km of river corridor length, which can provide advantages over purely empirical assessments (Pasternack, 2011). Detailed modeling enables sophisticated spatial analyses, which reveals biotic patterns and ecological functions that are space-dependent (Crowder and Diplas, 2000; Grantham, 2013; Pasternack et al., 2014), including emerging individual based bioenergetic modeling (Weber et al., 2006; Railsback et al., 2012; Hafs et al., 2014). Models can also analyze the ecohydraulics of potential river restoration designs, which data and empirical analyses cannot, since designed hydraulic conditions cannot be measured prior to construction (Bockelmann et al., 2004; Pasternack et al., 2004; Jacobson and Galat, 2006; Pasternack and Brown, 2013). River scientists, engineers, and restoration practitioners must understand the opportunities and limitations of different ecohydraulic modeling approaches (Brown and Pasternack, 2009; Pasternack and Senter, 2011; Jowett and Duncan, 2012).

Ecohydraulic models are often applied to decrease operational uncertainty in river assessment study or restoration design evaluation (Snowling and Kramer, 2001). Therefore, model selection negotiates technical, practical, and social tradeoffs to determine appropriate simulation complexity, optimizing the uncertainty reduction price point according to a cost-benefit analysis, either explicitly or unconsciously. Assessing benefits include estimating incremental uncertainty reductions offered by each modeling approach to select the approach commensurate with project's risks and resources (Gibson, 2013).

Spatially distributed depth and velocity maps are the most common hydraulic modeling product used as input for microhabitat modeling (Pasternack, 2011). Four approaches are available to develop these products: (i) 1D statistical modeling using transects, (ii) 1D hydraulic modeling, (iii) 2D hydraulic modeling, and (iv) 3D hydraulic modeling. However, the ecohydraulic literature mostly frames model selection as a choice between 1D statistical models and 2D numerical models (e.g., Sawyer et al., 2010), because most practitioners employ traditional transect data collection with statistical extrapolation (Payne and Bremm, 2003; Payne et al., 2004) whereas mechanistic ecohydraulic modelers have largely skipped over 1D hydraulic modeling to resolve spatial dependencies (Leclerc et al., 1995; Elkins et al., 2007). This work tests the hypothesis that 1D numerical models with lateral discretization algorithms represent a viable intermediate level of complexity for ecohydraulic analysis.

At least 18 comparisons of the results of 1D and 2D numerical models have been published in recent years to evaluate opportunities and limitations in environmental science and management applications (Ahmad and Simonovic, 1999; Waddle et al., 2000; Horitt and Bates, 2002; Werner, 2004; MacWilliams et al., 2006; Lee, 2006; Tayefi et al., 2007; Cook, 2008; Bohorquez and Darby, 2008; Alho and Aaltonen, 2008; Chatterjee et al., 2008; Brown and Pasternack, 2009; Clifford et al., 2010; Pasternack and Senter, 2011; Prestininzi et al., 2011; Leandro et al., 2011; Bladé et al, 2012; Jowett and Duncan, 2012). Though insightful, results were mixed (Gibson, 2013). In several studies, particularly large flood models with naturally orthogonal channel features at flood scales, 1D models performed well (Ahmad et al, 1999; Horitt and Bates, 2002; Gibson, 2005; Lee, 2006; Tayefi et al, 2007; Alho and Aaltonen, 2008; Jowett and Duncan, 2012). However, in highly complex non-orthogonal morphologies 1D results diverged from the 2D or 3D models (Waddle et al. 2000; MacWilliams et al. 2006; Lee, 2006; Brown and Pasternack, 2009). 1D models also under-performed in reaches with difficult-to-identify, non-orthogonal hydraulic controls that transects modeled poorly or missed all together (Pasternack and Senter, 2011). Thus, a key factor in selecting model dimensionality appears to be in the orthogonality and complexity of landforms present at scales and investigation needs to address.

Even with this extensive literature, two substantial data gaps complicate incremental uncertainty reduction comparisons between numerical 1D and 2D approaches:

1. Evaluating Laterally Discrete 1D Velocity Algorithms: Only five studies compared 1D and 2D velocities. Four compared 2D results with cross section averaged 1D model velocities (MacWilliams et al, 2006; Brown and Pasternack, 2009; Pasternack and Senter, 2011; Jowett and Duncan, 2012) and one study compared 2D results to lateral velocity data collected at a few locations, interpolated in one dimension (Waddle et al., 2000). None of the studies compared 2D models to “conveyance distributed 1D” velocity results, where cross section average velocities from 1D models are post processed to compute laterally explicit velocities, which represent ‘best practice’ for 1D velocity modeling.

2. Spatially Explicit Comparison of Depth and Velocity: Ecohydraulic applications require spatially distributed hydraulic depth and velocity results. To evaluate a 1D model for ecohydraulic analysis, 1D results must be translated into 2D depth and velocity grids and compared in this spatial framework. No spatially explicit comparisons of depth or velocity grids generated from 1D and 2D hydraulic model results were found. Additionally, most of the studies focused on comparing models for flood flows rather than for in-channel flows critical to ecohydraulic analysis. Revealing how spatial patterns change systematically as a function of discharge is important, because nonuniform channels exhibit flow-dependence of geomorphic processes (MacWilliams et al., 2006; Brown and Pasternack, 2014), habitat quality and abundance (Leclerc et al., 1995; Bovee et al., 1998), and interactions between the two (Pasternack et al., 2008; Hauer et al., 2011)

This study addressed these two data gaps, comparing spatially explicit, conveyance distributed 1D hydraulic model results against comparable 2D output. Depth and velocity maps were computed for three morphologically distinct reaches on the Yuba River, at three ecologically important flows with a 2D model and a conveyance distributed 1D. The model comparison addressed three specific research questions, each with hypotheses and test metrics (Table 1)**Error! Reference source not found.**.

2 Study Area

The Yuba River is a tributary of the Feather River, the north-eastern tributary of the Sacramento River, in northern California (Fig. 1). The river is topographically diverse and highly disturbed. The Yuba river watershed is 3,480 km^2 and includes contributing area from 10 m elevation valley floodplains to 2,774 m Sierra Peaks (Moir and Pasternack, 2008). This geographic diversity creates a down gradient morphological succession that was useful for this study. The river transitions from a steeper bedrock canyon (Pasternack et al., 2010) to valley-confined with braiding at wide sections (White et al., 2010), to anastomosing (where flood flows spread into multiple, relatively persistent channels), to meandering with moderate gradient, and, finally, to a confined, low gradient, leveed channel just upstream of its confluence with the Feather River in Marysville, CA.

The river also has a long history of disturbance including an early era (1850-1940) of placer, hydraulic and dredger gold mining, which left the system with a unique and recognizable aerial view and a complex story of sediment load and non-stationarity, followed by a later overlapping era (1910-present) of valley confinement by training berms, debris dams, and eventual, construction of the Englebright dam and consequent flow regulation. However, despite a complex history of landform and flow modifications, frequent overbank flooding and easily mobile alluvium have enabled the lower Yuba River to rapidly adjusted its flow-form dynamics to yield diverse landforms at morphological unit to segment scales (Carley et al., 2012; Wyrick and Pasternack, 2012, 2014). The river supports a diverse fish community (Kozlowski, 2004) and is widely viewed as a lynchpin to maintaining and restoring the salmonid meta-populations in the northern Central Valley region (YARMT, 2013).

3 Methods

Three geomorphologically distinct reaches (channelized, meandering, and anastomosing) of the lower Yuba River were modeled at three flows (20% of bankfull discharge, bankfull, and four times bankfull) with the one-dimensional hydraulic model HEC-RAS (USACE, 2010) and the two-dimensional hydraulic model SRH-2D (Lai, 2008; Pasternack, 2011). Modeling specialists applied each model to assure ‘skill control’ and remove asymmetrical modeler ability as a confounding variable. Both modeling efforts began with the same raw bathymetry data and specified flows, applying best modeling practice for 1D and 2D approaches without reference to the approach or results of the other. HEC-RAS and the GIS post-processor HEC-GeoRAS (USACE, 2009) generated two dimensional depth and velocity grids for each of the nine conditions (three reaches at three flows) from the 1D results. These grids were then compared to the results of an existing, validated two-dimensional SRH-2D model of the lower Yuba River (Barker, 2011; Abu-Aly et al., 2013; Pasternack et al., 2014) to quantify the error introduced by the 1D assumptions. Errors were reported in a flow-reach morphology matrix. Although the 2D model was heavily tested for uncertainty using traditional and novel validation tests, validation data were not collected with the intention of calibrating and validating a 1D model independently; this study is an opportunistic scientific exploration involving model comparison to better understand modeling practices and trade-offs.

3.1 Reach Selection

Reaches were selected from a detailed river corridor digital elevation model (DEM) of the lower Yuba, constructed using a combination of ground-based, boat-based, and remote sensing methods (Carley et al., 2012; Pasternack et al., 2014). For the lowermost 28.3 km of the river from which the three study reaches herein were selected, the overall mean subaqueous grid point spacing within the 24.9 m^3/s wetted area was one point every 1.3 m. (59.8 pts/100 m^2)- though with patches having larger gaps where data collection was hazardous or otherwise difficult- while for the subaerial river terrain at that flow the overall mean grid point spacing was one point every 0.43 m. (554 pts/100 m^2). This point density was sufficient to capture the roles of sub-width topographic nonuniformity on hydraulic modeling.

Based on the multi-scalar landform assessment study of Wyrick and Pasternack (2012), three morphologically distinct reaches were selected (Table 2). Reach 1 is a low gradient, confined, urban, leveed channel. Upstream about 4 km, Reach 2 is a moderate gradient meandering section with alternate point bars. Reach 3 is an anastomosing reach with multiple parallel channels and additional side channels at higher flows. Upstream reaches included more backwater zones, floodplain connectivity, flow splits, hydraulic roughness, hydraulic separation zones, steeper slopes, and morphological diversity. While no single metric explains the morphological gradient in a simple monotonic trend, the progression of the combined metrics along Reach 1→Reach 2→Reach 3 fits a gestalt impression of increasing “complexity.” However, because of the unhelpful connotations and semantic range of the term complexity, trends will be described in reference to ‘gradient’ (where Reach 1 is down gradient and Reach 3 up gradient), with basic downstream (Reach 1) to upstream (Reach 3) terminology or single thread (Reach 1 and 2) versus multi-thread (Reach 3) when appropriate.

3.2 The 2D Model

This study utilized output from an existing 2D model of the Yuba River developed by co-author Pasternack in collaboration with the Yuba Accord River Management team. Barker (2011) and Pasternack et al. (2014) described the full details of model development and testing. The 2D model was heavily scrutinized through by scientists, and managers, and is now used for diverse applications in both arenas. SRH-2D (Lai, 2008) was used to model ~35 km of the lower Yuba River, from the Englebright Dam to the confluence with the Feather River, except for a ~ 2-km section with unmapped rapids in The Narrows bedrock canyon. The mixed structured-unstructured computational mesh had a typical intermodal spacing of 0.91 to 1.5 m for base and bank full flow and a near uniform 3 m mesh for flood flows.

The 2D model was validated (Barker, 2011) using independent datasets for water surface elevations, depths, and velocity magnitude and direction collected over a range of discharges (~14 to 170 m^3/s). A few performance metrics are provided herein with the full analysis available in Barker (2011). Model mass conservation was within 1%. Mean, signed, water surface elevation residual was −1.8 mm for 197 observations at 24.92 m^3/s. For unsigned residuals, 27% were within 3.1 cm, 49% were within 7.62 cm, 70% within 15.25 cm, and 94% within 30.5 cm. Depth observations from cross section surveys yielded a good coefficient of determination (R^2) of 0.66 (n=199). Barker (2011) measured velocity magnitude using two different ways to make a robust validation analysis - one with a traditional cross-section approach suitable for a small number of observations with high accuracy and one using a new approach involving Lagrangian particle tracking. For the former approach, 40-s average velocity magnitude was measured at the standard 0.6·depth vertical position for the same 199 points where depth was observed along traditional cross-sections with either a Marsh-McBirney® Flo-Mate electromagnetic current meter sampling at 30 Hz or a Price AA mechanical impellor current meter. However, for assessing 2D model performance for 33-km of channel over an order of magnitude of flows, the traditional method should be balanced by a rapid observation strategy that provides far more data. Therefore, the Lagrangian surface velocity vector tracing method of Stockdale et al., (2007) was improved upon by switching from differential GPS to real-time kinematic GPS and from unattended floats to a manned kayak wherein one may carefully insure that the kayak adheres to the direction and magnitude of velocity. As the kayak moves with the flow, positions are measured with ~ 0.02-0.05 m accuracy every 5 s and then these positions are differenced over that time interval to yield surface velocity magnitude, which is assigned to the midpoint between each adjacent pair of position observations. Surface velocities are next converted to depth-averaged values using the proper regression equation for the two established for the river. Although this adds some uncertainty for each point, one can measure thousands to tens of thousands of velocities per day covering many kilometers of channel, so the statistical robustness of the predicted versus observed regression relation is far greater compared to that when only a few hundred points are used, yielding an overall superior validation assessment. Methodological details are explained in the ecohydraulics textbook by Pasternack (2011). Using this method, the 2D model yielded an R^2 of 0.79 between predicted and observed. Median unsigned velocity magnitude error was 16%, significantly smaller than commonly reported (Wyrick and Pasternack, 2014; Brown and Pasternack, 2014).

The SRH-2D model was used to analyze three ecologically interesting flows in this study: base (28 m^3/s), bankfull, (142 m^3/s), and floodplain filling (597 m^3/s) flows – events with >99, 83, and 40% annual exceedance probabilities, respectively. Even though Abu-Aly et al. (2013) developed and published on a meter-scale spatially distributed Manning's n scheme using relative surface roughness (i.e., ratio of vegetation canopy height to water depth) obtained from LiDAR data, for this study model runs that exclusively had a universal Manning's n-value (0.04) were used to remove spatial roughness distribution as a confounding variable from the comparison instead of the more complex vegetated models used for the final Yuba analysis. In cases where complex vegetation patterns are present and important to the ecohydraulic problems in question, this could be a deciding factor to use a 2D model and the scheme of Abu-Aly et al. (2013).

3.3 The 1D Model

HEC-RAS models were developed for the three selected reaches. A thalweg shape file, computed during the 2D modeling, became the stream center line and HEC-GeoRAS was used to cut cross sections from the TIN used for the 2D model every one-to-two channel widths. Each reach was initially modeled with a single computational reach in the 1D model (i.e. no flow splits). The base n-value (0.04) from the 2D model was applied to the channel and over banks in the 1D model. However, it is common practice (Brickler et al., 2014) to calibrate 1D n-values to multiple flows, specifying flow dependent adjustments to the roughness parameters. Therefore, water surface elevations were extracted from the 2D simulations at the intersection of every other cross section and the stream center line. The "flow roughness factors" in HEC-RAS were adjusted to calibrate the 1D water surface elevations to the 2D water surface elevations. Factors used and the resulting residuals are included in **Error! Reference source not found.** and

Table 4.

An experienced 1D modeler might identify Reach 3 as a good candidate for a 'split flow' 1D modeling approach. Split flow modeling is actually an intermediate level of complexity between 1D and 2D modeling with intermediate costs and parameterization demands. Although a full presentation is beyond the scope of this article, Reach 3 was also modeled with a split flow 1D approach (Fig.3). Split flow results were compared to the single reach results (Gibson, 2013).

3.4 Computing Spatially Explicit Velocity Maps From 1D Results

Traditionally ecohydraulics involved sampling-based statistical analysis of hydraulic conditions to quantify the statistical relationships between discharge and weighted usable area (Payne et al., 2004). However, ecohydraulics has shifted toward a spatially explicit characterization of habitat in the last decade, with meter-scale prediction of both presence and absence of biotic habitat utilization (e.g., Elkins et al., 2007). As a result, ecohydraulic literature addressing scientific exploration of spatial physical-biotic linkages and meter-scale habitat predictions often dismiss 1D models, because cross section averaged velocities cannot achieve these outcomes. However, HEC-RAS includes analytical methods that compute lateral velocity distributions from cross section averaged results and translates these into velocity maps, which are rarely discussed in ecohydraulic literature and have never been evaluated relative to the results of 2D or 3D models. These methods are widely available in public domain software and include, (i) post processing 1D cross section averaged velocities analytically to compute lateral velocity distributions at each cross section and (ii) spatial interpolation of these laterally discrete velocities based on the Laplace equation to compute a smooth 2D velocity map that follows logical flow paths.

3.4.1 Analytical Lateral Velocity Distributions

After computing cross section averaged velocities to determine water surface elevations, HEC-RAS uses conveyance principles to compute a lateral velocity distribution at each cross section (Fig. 3). The algorithm uses Manning's equation to partition the 1D cross-section velocity into up to 45 laterally discrete 'flow prisms' across the cross section. The non-linearity of Manning's equation generates non-additive conveyance weighted velocities, so the algorithm initially computes a weighted sum of the prism velocities that does not match the 1D cross section velocity. Therefore, after the distributed velocities are computed, they are scaled to ensure the weighted average velocity is the same as the overall velocity computed by the 1D analysis, conserving cross section conveyance (USACE, 2010).

3.4.2 Interpolating and Mapping Velocity

Once lateral velocity distributions are computed at each cross section, a second algorithm translates those results into a 2D velocity grid that can be compared to 2D model results. Interpolating a simple TIN from a velocity point shape file produces noisy velocity maps with spurious results, particularly in meandering channels. Therefore, HEC-GeoRAS includes algorithms that guide inter-cross section velocity interpolation.

HEC-RAS computes the centroid of each flow prism and assigns coordinates to the prism velocity, generating an x, y, velocity geodatabase. Then HEC-GeoRAS uses the Laplace equation to develop smooth, curvilinear, transitional streamlines between the stream centerline, the river banks, and the flood boundary (excluding any ineffective flow areas) to guide velocity interpolation between cross sections according to physically reasonable flow paths. The laterally explicit, analytical velocity distribution and the Laplacian interpolation produce a 2D velocity grid from the 1D velocities that can be compared to 2D results.

These methods for converting 1D results into a 2D velocity grid are approximate, *ad hoc*, and empirical. But they represent 1D velocity mapping 'best practices' and there is no detailed published attempt to rigorously evaluate their performance. Evaluating their performance on ecohydraulic scales is the primary objective of this work. The combined effects of the conveyance weighted subdivision of the 1D-cross section averaged velocity and the Laplacian mapping approach with be referred to as "conveyance distributed 1D" velocity results, for simplicity.

3.5 Evaluation Metrics

For each reach and flow, the 1D depth and velocity grids were superimposed on the 2D grids. One-dimensional results at each cell were plotted against 2D result and the coefficient of determination (R^2) was computed for each scenario. Additionally, residuals (ε) were computed for each cell, where:

$$\varepsilon = \frac{1D_{result}-2D_{result}}{2D_{result}} \tag{1}$$

(Clifford et al., 2005) and the "median absolute residual" ($|\tilde{\varepsilon}|$) was computed to summarize the residuals of each scenario into a single parameter. Velocity residuals were also mapped for each reach and flow to provide context for the summary statistics and generate spatial intuition. Both metrics were used to evaluate results in order to escape analysis artifacts that emerge from the limitations of either statistic, and support conclusions independent of the individual liabilities of each metric.

4 Results

4.1 How well does a 1D model replicate 2D depth results?

The 1D model predicted depths well by both test metrics. The 1D depth predictions were more reliable downstream and at higher flows (Table 5; Fig. 4). All reaches and flows returned $R^2 \geq 0.94$ ($R^2_{mean}=0.98$ and $R^2_{median}=0.99$) and median absolute residuals were all $|\tilde{\varepsilon}| \leq 7.2\%$ (i.e. 50% of residuals are approximately within ±3.6% for the worst case). Additionally the flood flows returned $R^2 \geq 0.99$ and median absolute residuals $|\tilde{\varepsilon}| \leq 4.0\%$ (i.e. 50% of residuals are approximately within ±2.0%) for all reaches.

4.2 How well does a conveyance distributed 1D model replicate 2D velocity results?

Velocity residuals were larger and R^2 smaller than depth results (Table 6; Fig.5). Coefficients of determination for velocity results fell between $0.42 \leq R^2 \leq 0.81$, ($R^2_{mean}=0.70$ and $R^2_{median}=0.73$). Median absolute velocity residuals ($|\tilde{\varepsilon}|$) were substantially larger and less sensitive to flow and reach type than depth results, including the range $9.6\% \leq |\tilde{\varepsilon}| \leq 22.4\%$ (approximately ±4.6 to 11.2%) with means and medians of $|\tilde{\varepsilon}|_{maan}=14.2\%$ and $|\tilde{\varepsilon}|_{median}=13\%$.

Velocity residual trends were not as easily interpreted as those for depth. R^2 increased monotonically with depth for the meandering and anastomosing reaches (Reaches 2 and 3) but decreased with flow for the channelized reach (Reach 1). Alternately, the bankfull flow returned the minimum median absolute residual for each reach, while the maximum residual was associated with the base flow for Reaches 1 and 3 and flood flow for Reach 2. Additionally, Reach 2 had the highest median absolute residual (for flood flow) and the lowest R^2 (for base flow), both precluding monotonic trends by gradient. Flood flow residuals make more sense in their spatial context, discussed below, but the unusually low R^2 associated with the Reach 2 base flow helps categorize these results in the absence of generalized trends.

Two of the nine scenarios had R^2 substantially lower than the others: base flow for the meandering and anastomosing reaches (Reaches 2 and 3). Upon closer inspection, these conditions represent similar processes and can be grouped. The “meandering reach” does, in fact, meander for high flows. However, Reach 2 at base flow, the condition with the lowest R^2, includes three substantial flow splits affecting 30% of total reach length (versus 48% of the ansatomosing reach at base flow), making Reach 2 an anastomosing reach at base flow. Therefore the data can be stratified by this condition. The model performed poorly for anastomosing base flows ($0.42<R^2<0.58$) but performed better and more consistently, ($0.69 < R^2 < 0.81$, $R^2_{mean}=0.75$ and $R^2_{median}=0.77$) for all other conditions.

4.3 What Hydraulic processes generate large velocity residuals?

Velocity residuals were larger and more spatially interesting than depth results. Therefore, the residual maps for each flow in Reach 1, Reach 2, and Reach 3 are included in Figures 6, 7, and 8 respectively. The convention of Blue for negative (2D>1D) and red for positive (1D>2D) residuals is used throughout. The largest velocity residuals were associated with backwater zones (2D>1D) and in the separation zones downstream of outcrops, islands and bouleers (1D>2D). The analysis also returned substantial residuals in side channels and flow separation zones. The multi-channel complex in the downstream section of Reach 3, which transitions between backwater at low flows to active flood conveyance at flood flows was also a region of particularly high residuals. Finally, where the models predicted overbank flooding, the 1D model consistently over-predicted velocity in the channel and under predicted velocity in the floodplain in all three reaches.

4.4 Split Flow Results

Split flow modeling results were mixed. The summary statistics (R^2 and $|\tilde{\square}|$) are reported in Table 7. The split flow model improved depth R^2 and residuals for all flows. R^2 improvements were substantial for base flow (0.89 to 0.96) but $|\tilde{\square}|$ improvements were much more modest (0.2-1.1%). Stratifying residuals spatially revealed a more complex story.

In the classic, persistent split flow region of Reach 3 (the “Long Bar” in Fig.3), the split flow model dropped residuals substantially, approximately halving $|\tilde{\square}|$ for each flow. However, in the multi-reach complex at the downstream end of the model Fig.3), where channels transitioned from dry, to backwater zones, to conveying reaches in different models, split flow modeling did not substantially improve depth results and, in some cases increased residuals.

The split flow model also increased velocity R^2 for all flows, sometimes substantially, particularly for the problematic base flow anastomosing conditions (Reaches 2 and 3 at the lowest flow), raising R^2 above the 0.7 threshold for all reaches. However, split flow effects on velocity residuals were more modest and not universal. Split flow improved 1D residuals a little (2.1 to 2.2%) for the base flow bank full condition, but not for flood flow (where $|\tilde{\square}|$ decreased by 1.1%). These trends also obtained for the long bar region, where velocity residuals dropped substantially for bank full flow, but modestly for base flow and increased for flood flow.

5 Discussion

5.1 Process Discussion

The highest depth residuals occurred in zones where the 1D assumptions broke down (Fig.9), like side channels, backwaters, separation zones, and around islands. The 1D model requires a single water surface elevation across the channel, while side channels and backwaters can maintain distinct water surface elevations, generating 1D depth residuals. The 1D model also overpredicted depth downstream and underpredicted depth upstream of obstructions like islands, where localized momentum effects cause stage depression and super elevation respectively, which the 1D model does not simulate.

Some of these depth divergence features translated directly into velocity divergence. Overpredicting flow in side channels led and under predicting flow in backwaters generating velocity residuals that were larger than the corresponding depth residuals, consistent with Pasternack et al.'s (2006) finding that errors amplify as they propagate through depth, velocity, and shear computations respectively.

Velocity residuals upstream of islands diverged from depth residuals. Super elevation upstream of islands did not translate into appreciable velocity residuals above background. However, velocity residuals downstream of islands were much larger than depth residuals. Velocity residuals around an island in Reach 2 were rescaled in Fig.10 to illustrate the region of maximum divergence (>100%). However, the most egregious residuals mapped within the 2:1 expansion zone, which represents the 'rule of thumb' criteria for designating an 'ineffective flow area' to model a non-conveying zone downstream of an obstacle in a 1D model (HEC, 1995; USACE, 2010).

Finally, the 1D model tended to overpredict channel velocity and under predict floodplain velocity, implying that the conveyance assumption used in lateral velocity distribution is not complete, and includes simplifications that introduce bias. These trends obtain in the flood flow results of each reach and are responsible for the particularly high residuals for the flood flow of Reach 2, the condition with the most flood plain area. However, they are best illustrated in the relatively simple single bar in from Reach 1 (Fig.11), where there are fewer confounding influences. While the 1D model discretizes flow laterally, based on conveyance, it does not account for viscous losses or momentum transfer between these lateral flow prisms. Therefore, the conveyance distributed, 1D approach tends to overpredict velocities for the deepest prisms with the most inter-prism surface area for lateral momentum exchange. When individual prism velocities are normalized to make the flow average velocity match the 1D cross section velocity, overbank velocities are reduced to compensate for over predicted velocities in the channel, making them under predict. This result is anecdotal and cannot necessarily be generalized. But it highlights an artifact of the analytical lateral velocity distribution that will cause 1D results to diverge from 2D velocities. This would have serious implications if this lateral distribution scheme were used for ecohydraulic analysis of flood refugia, avulsion or toe scour. Even when 1D models like HEC-RAS compute edge effects like toe scour, they post process 1D shears with *ad hoc* radial shear partitions, to compute a vertical shear distribution similar to the lateral 'conveyance distributed' velocity partition (Gibson *et al*. 2015).

The complex relationship of velocity residuals highlights an advantage of 2D models in multi-channel analysis: 'generality.' A 1D split flow model must be designed for a particular flow, in this case, the bank full flow, which is why the split flow improvements were greatest for bank full flow, for both model as a whole and the long bar in particular. The 1D flow split is determined *a priori* for a particular flow, which introduces error in higher and lower flows (Fig.12). This cross section lay out separates conveyance at river stations that are connected at higher flows and artificially connects channels that are separated at lower flows, while a 2D modeling domain has the property of *generality*, customizing the flow split around the island for each discharge. A 1D model can mitigate these effects with a lateral structure to model flow exchange over the bar, but adding a lateral structure adds complexity to the 1D model and did not appreciably improve the basic velocity residual trend in this case.

5.2 Interpretive Implications of Uncertainty in 2D results

The above analysis treats the 2D model results as ground truth and evaluates the 1D model based on its ability to reproduce them. However, model evaluation theory often recognizes the implications of ground truth data uncertainty in the process of model evaluation. 2D models of gravel/cobble bed rivers have assumptions and limitations as well. Both roughness parameterization and turbulence closure are well known problems afflicting the type of model used herein. Similarly, 2D model assumptions break down in meanders and steep rapids, both of which occur in the modeled reaches, though the resulting loss in accuracy with decreasing suitability of the assumptions is not well illustrated in the literature. Further, the 2D model assumes a no slip boundary along the bed, but because the bed is highly porous this is not true. In terms of limitations, airborne LiDAR mapping of subaerial terrain and single-beam echosounder mapping of subaqueous terrain have high uncertainty relative to the precision of model predictions and thus accurate topography remains the key limitation as well understood from past studies (Anderson and Bates, 1994; Marks and Bates, 2000; Pasternack et al., 2006).

Both the number of velocity validation observations and the goodness of fit in the 2d LYR model were among the highest ever reported for a 2D velocity calibration (Wyrick and Pasternack, 2014), plus this study was among the rare few that actually evaluated velocity direction. For the base flow anastomosing reaches (Reaches 2 and 3 for the lowest flow) the performance of the 1D model, as indicated by the velocity R^2, was underwhelming ($0.42<R^2<0.58$), substantially less than the implicit uncertainty of the 2D model. However, the 2D model's uncertainty ($R^2=0.784$) is comparable to that observed between 1D and 2D results in the other seven reach-flow pairs ($R^2_{mean}=0.75$ and $R^2_{median}=0.77$).

Several classical model evaluation metrics reduce the residual by the uncertainty of the observed data, including Relative Mean Absolute Error (RMAE) such that:

$$RMAE_{Depth} = \frac{|H_c - H_m| - \Delta H_m}{H_m} \quad \text{and} \quad RMAE_{Vel} = \frac{|V_c - V_m| - \Delta V_m}{V_m} \qquad (2)$$

where H_c is computed depth, H_m is measured depth, V_c is computed velocity, V_m is measured velocity and DH_m and DV_m are the error in the measured depth and velocity respectively. In this case, where the 1D is the computed and 2D is 'measured' the analogy would be:

$$RMAE_{Depth} = \frac{|H_{1D} - H_{2D}| - \Delta H_{2D}}{H_{2D}} \quad \text{and} \quad RMAE_{Vel} = \frac{|V_{1D} - V_{2D}| - \Delta V_{2D}}{V_{2D}} \qquad (3)$$

RMAE assumes that the residuals between the 1D and 2D model and the 2D model and the velocity observations are uncorrelated, and, therefore, on average, counteracting. In this case, considering the uncertainty in the 2D could improve the relative results of the 1D model in comparison. However, if these residuals (1D vs 2D and 2D vs measured) are correlated, then they will be additive, decreasing the value of the 1D results. Because physical observations spanned the entire lower Yuba, there were not enough in the considered reaches to incorporate 2D residuals explicitly in 1D-2D comparison. However, it is worth noting that outside of base flow for anastomosing reaches, the 1D to 2D comparisons generated R^2s on the order of the 2D to measurement comparisons. Overall, more systematic studies that evaluate the performance of 1D and 2D models with incrementally greater degrees of violation of assumptions would benefit the understanding and application of hydraulic models.

5.3 Non-Statistical Implications for Model Selection

The discussion above provides data on the 'benefit' side of a cost-benefit approach to model selection. It presumes that moving from a 1D to a 2D model represents a substantial and easily quantifiable cost increase (usually in the form of bids or scope of work proposals), that can now be compared to the benefit of incremental uncertainty reduction for a matrix of morphologies and flows documented in Fig.Figure 4, Table 5, Fig.5, and

Table 6

However, there are at least two, non-statistical considerations that should frame these results and their application to a cost-benefit approach to model selection:

1. The 1D model used tight cross section spacings in this study, on the order of 1 to 2 channel widths. These are not unusual if a complete digital elevation model, including both channel and overbank bathymetry, exists (Kootenai Tribe, 2014; Shelley and Gibson, 2015; USACE, 2009; Bales et al., 2007). The cost of cutting new cross sections on a digital landscape is minor, though because automated methods are still not recommended, it does increase effort. However, acquiring a detailed, "near-census" (i.e., meter-scale) bathymetry is often the primary cost of 2D modeling. Near-census bathymetry can be used for many purposes beyond just the 2D model study, so more river managers are collecting it. On the other hand, in the absence of near-census bathymetry, 1D models can have problems if important hydraulic controls in the river are not known *a priori* or are known but are not assigned cross-sections. This can happen if the controls are underwater and difficult to see, especially for long reaches with poor accessibility. The incremental cost of moving from a 1D to a 2D model can be small compared to the cost of acquiring detailed bathymetry. This 1D-2D comparison presumes that detailed bathymetry already exists and does not inform a common decision between modeling the system with a 1D model based on existing, surveyed, widely spaced cross sections and investing in the bathymetry to make a 2D model possible. As the incremental cost of moving from a 1D to a 2D model decreases, a thinner uncertainty reduction (benefit) justifies moving to the 2D model.

2. This study controlled for modeler skill by entrusting the 1D and 2D modeling to specialists. However, 2D models handle more of the physics explicitly and, therefore, require fewer modeling 'tricks' and subjective modeling decisions (e.g. bank stations, flow split locations, and ineffective flow areas in a multi-reach complex). 1D modeling is more sensitive to modeler decisions, making the simpler model, counter intuitively, more sensitive to modeler skill. Therefore, 1D model results are more variable than 2D results. Vulnerability to user variability (Dawdy and Vanoni, 1986) adds to 1D uncertainty in ways this study did not capture.

6 Conclusions

This study compared results from conveyance distributed 1D depth and velocity modeling, including analytical lateral velocity computations and Leplacian mapping algorithms for inter-cross section mapping, to 2D results for three flows in three morphologically distinct reaches.

The 1D goodness of fit was between $0.94 \geq R^2 \geq 1.00$ (R^2_{mean}=0.98 and R^2_{median}=0.99) for depth and median absolute residuals were all $3.8 \leq |\tilde{\epsilon}| \leq 7.2\%$ (i.e. 50% of residuals are approximately within ±1.7 to ±3.6%). Higher flows and lower gradient reaches with fewer side channels and backwaters had lower depth residuals.

The velocity goodness of fit fell between $0.42<R^2<0.81$, but the anastomosing base flows were much worse ($0.42<R^2<0.58$) than the other seven conditions ($0.69 < R^2 < 0.81$, $R^2_{mean}=0.75$ and $R^2_{median}=0.77$). Velocity residuals were substantially higher than depth residuals, spanning $9.6\% > |\tilde{\square}| > 22.4\%$ (e.g. 50% of the residuals fell approximately between ±4.6% for the best 1D model and ±11.2% for the worst) with means and medians of $|\tilde{\square}|_{maan}=14.2\%$ and $|\tilde{\square}|_{median}=13\%$ (50% of residuals falling within approximately ±7.1 and ±6.5% respectively). The highest residuals were concentrated in backwaters, flow separation zones, island velocity shadows, side channels, complex, and multi-reach reaches, particularly where some reaches transition between backwater to conveyance as flow increases. Additionally, the 1D analytical lateral velocities algorithm consistently over predicted velocity in the channel and under predicted velocity in the flood plain. While split flow improved depth results substantially (~50%) in a classic bifurcation situation, it was less effective in a multi-channel complex and did not improve velocity results substantially or universally. Opportunities for additional research include evaluating the sensitivity of conveyance weighted modeling results to the number of prisms (initial investigation suggest rapid diminishing returns for more than three to five prisms) and translating the error incurred by selecting a simplified model into some measure of project risk.

Many comparisons of 1D and 2D models return conclusions that the latter are better than the former (Bohorquez and Darby, 2008; Tayefi et al., 2007; Brown and Pasternack, 2009; Prestininzi et al., 2011), that model results are comparable (Alho and Aaltonen, 2008; Horitt and Bates, 2002) or, sometimes, that a particular 1D model outperformed a particular (usually gridded) 2D model for a particular situation (Jowlett and Duncan, 2012; Gibson, 2005). But this is not the most useful model selection question. The pertinent management question is not, “is a 2D model better than 1D model?” A well constructed, high resolution, multi-dimensional model with comparable features (e.g. algorithms to simulate hydraulic structures) should outperform a 1D model constructed at a comparable scale with comparable expertise.

Instead, the pertinent questions are “how much better is the 2D answer than the 1D answer?” and “does the risk reduction achieved by selecting 2D justify upgrading from the 1D option?” A cost benefit analysis between levels of modeling complexity requires quantifying benefits to compare to the costs. This work helped quantify those benefits, the incremental uncertainty reductions of moving from a 1D to 2D modeling framework, to allow explicit cost-benefit approaches to model selection.

7 Acknowledgments

This project benefitted from work done with funding provided by the Yuba County Water Agency and the Yuba Accord River Management Team (Award #201016094). Funding for G.B. Pasternack was provided by the USDA National Institute of Food and Agriculture, Hatch project number #CA-D-LAW-7034-H. Funding for S.A. Gibson was provided by the Corps of Engineers

Flood and Coastal Storm Damage Reduction R&D Program. Lily Tomkovic generated the black and white maps and figures for hard copy publication.

8 References

Abu-Aly TR, Pasternack GB, Wyrick JR, Barker R, Massa D, Johnson T. 2013. Effects of LiDAR-derided, spatially-distributed vegetative roughness on 2D hydraulics in a gravel-cobble river at flows of 0.2 to 20 times bankfull. *Geomorphology*. doi:10.1016/j.geomorph.2013.10.017.

Ahmad S and Simonovic SP. 1999. Comparison of One-Dimensional and Two-Dimensional Hydrodynamic Modeling Approaches For Red River Basin. Natural Resources Institute Facility for Intelligent Decision Support. University of Manitoba, Winnipeg, Manitoba : 51.

Alho P and Aaltonen J. 2008. Comparing a 1D hydraulic model with a 2D hydraulic model for the simulation of extreme glacial outburst floods. *Hydrological Processes* **22(10)** : 1537-1547.

Anderson MG and Bates PD. 1994. Evaluating data constraints on two-dimensional finite element models of floodplain flow. *Catena* **22** : 1–15.

Barker JR, Pasternack GB, Bratovich P, Massa D, Reedy G, Johnson T. (2011), Method to Rapidly Collect Thousands of Velocity Observations to Validate Million-Element 2D Hydrodynamic Models, in AGU, edited, San Francisco.

Barker JR. 2011. Rapid, abundant velocity observation to validate million-element 2D hydrodynamic models. M.S. Thesis, University of California at Davis, Davis, CA.

Bales JD, Wagner CR, Tighe KC, Terziotti S. 2007, LiDAR-derived flood-inundation maps for real-time flood-mapping applications, Tar River basin, North Carolina. *U.S. Geological Survey Scientific Investigations Report 2007–5032*.

Bladé E, Gómez-Valentín M, Dolz J, Aragón-Hernández JL, Corestein G, Sánchez-Juny M. 2012. Integration of 1D and 2D finite volume schemes for computations of water flow in natural channels. *Advances in Water Resources* **42** : 17-29.

Bohorquez P and Darby SE. 2008. The use of one- and two-dimensional hydraulic modeling to reconstruct a glacial outburst flood in a steep Alpine valley. *Journal of Hydrology* **361(3-4)** : 240-261.

Bockelmann BN, Fenrich EK, Lin B, Falconer RA. 2004. Development of an ecohydraulics model for stream and river restoration. *Ecol. Eng* **22(4–5)** : 227-235.

Bovee KD, Lamb BL, Bartholow JM, Stalnaker CB, Taylor J, Henriksen J, 1998. Stream habitat analysis using the instream flow incremental methodology. USGS/BRD-1998-0004, United States Geological Survey, Fort Collins, CO.

Brickler JD, Gibson SG, Imamura F, Takagi H. 2014. On the Need for Larger Manning's Roughness Coefficients in Tsunami Inundation Models. *Journal of Coastal Engineering*, In Review.

Brown RA and Pasternack GB. 2014. Hydrologic and topographic variability modulate channel change in mountain rivers. *Journal of Hydrology* **510** : 551-564.

Brown RA, and Pasternack GB. 2009. Comparison of methods for analyzing salmon habitat rehabilitation designs for regulated rivers. *River Research and Applications* **25(6)** : 745-772.

Carley JK, Pasternack GB, Wyrick JR, Barker JR, Bratovich PM, Massa DA, Reedy GD, Johnson TR. 2012. Significant decadal channel change 58-67 years post-dam accounting for uncertainty in topographic change detection between contour maps and point cloud models. *Geomorphology*. doi:10.1016/j.geomorph.2012.08.001.

Chatterjee C, Förster S, Bronstert A. 2008. Comparison of hydrodynamic models of different complexities to model floods with emergency storage areas. *Hydrological Processes* **22(24)** : 4695-4709.

Clifford NJ, Soar PJ, Harmar OP, Gurnell AM, Petts GE, Emery JC. 2005. Assessment of hydrodynamic simulation results for eco-hydraulic and eco-hydrological applications: a spatial semivariance approach. *Hydrological Processes* **19(18)** : 3631-3648.
Clifford NJ, Wright N, Harvey G, Gurnell AM, Harmar OP, Soar PJ. 2010. Numerical Modeling of River Flow for Ecohydraulic Applications: Some Experiences with Velocity Characterization in Field and Simulated Data. *Journal of Hydraulic Engineering* **136(12)** : 1033-1041.
Cook A. 2008. Comparison of one-dimensional HEC-RAS with two-dimensional FESWMS model in flood inundation mapping. Purdue University, West Lafayette, Indiana.
Crowder DW and Diplas P. 2000. Using two-dimensional hydrodynamic models at scales of ecological importance. *Journal of Hydrology* **230** : 172-191.
Dawdy DR and Vanoni VA. 1986. Modeling Alluvial Channels. *Water Resources Research* **22(9)** : 71-81.
Elkins EE, Pasternack GB, Merz JE. 2007. The Use of Slope Creation for Rehabilitating Incised, Regulated, Gravel-Bed Rivers. *Water Resources Research* **43**, W05432, doi:10.1029/2006WR005159.
Gibson S, Simon A, Langendoen E, Bankhead N, Shelley J. 2015. A Physically-Based Channel-Modeling Framework Integrating HEC-RAS Sediment Transport Capabilities and the USDA-ARS Bank-Stability and Toe-Erosion Model (BSTEM). Federal Interagency Sediment Conference, SedHyd Proceedings.
Gibson S. 2005. Unsteady HEC-RAS Model of the Downtown Reach of the Truckee. U.S. Army Corps of Engineers - Hydrologic Engineering Center. 39.
Gibson S. 2013. Comparing Depth and Velocity Grids Computed With One- and Two-Dimensional Models at Ecohydraulic Scales. M.S. Thesis, University of California at Davis, Davis, CA.
Grantham TE. 2013. Use of hydraulic modeling to assess passage flow connectivity for salmon in streams. *River Research and Applications* **29** : 250–267. doi: 10.1002/rra.1591
Hafs AW, Harrison LR, Utz RM, Dunne T. 2014. Quantifying the role of woody debris in providing bioenergetically favorable habitat for juvenile salmon. *Ecol. Model* **285(0)** : 30-38.
Hauer C, Unfer G, Tritthart M, Habersack H. 2011. Effects of stream channel morphology, transport processes and effective discharge on salmonid spawning habitats. *Earth Surf. Process. Landforms* **36** : 672–685. doi: 10.1002/esp.2087
HEC. 1995. Flow Transitions in Bridge Backwater Analysis, Hydrologic Engineering Center, Davis, CA.
Horritt M and Bates PD. 2002. Evaluation of 1D and 2D numerical models for predicting river flood inundation. *Journal of Hydrology* **268**: 87-99.
Jacobson RB and Galat DL. 2006. Flow and form in rehabilitation of large-river ecosystems – an example from the lower Missouri River. *Geomorphology* **77** : 249-269.
Jowett IG and Duncan MJ. 2012. Effectiveness of 1D and 2D hydraulic models for instream habitat analysis in a braided river. *Ecological Engineering* **48** : 92-100.
Kootenai Tribe of Idaho. 2014. Kootenai River Habitat Restoration Program Flood Risk Analysis and Compliance Report : 255.
Kozlowski JF. 2004. Summer Distribution, Abundance, and Movements of Rainbow Trout (Oncorhynchus mykiss) and other Fishes in the Lower Yuba River. University of California, Davis, CA, California : 88.
Lai YG. 2008. SRH-2D Version 2: Theory and User's Manual. U.S. Department of the Interior, Bureau of Reclamation, Technical Service Center, Denver, CO.

Leandro J, Djordjević S, Chen AS, Savić DA, Stanić M. 2011. Calibration of a 1D/1D urban flood model using 1D/2D model results in the absence of field data. *Water Science & Technology* **64(5)** : 1016.

Leclerc M, Boudreault A, Bechara JA, Corfa G. 1995. Two-dimensional hydrodynamic modeling: a neglected tool in the instream flow incremental methodology. *Transactions of the American Fisheries Society* **124** : 645–662.

Lee K. 2006. Comparison of the Theory, Application, and Results of One- and Two-Dimensional Flow Models. Auburn : 129.

MacWilliams ML, Wheaton JM, Pasternack GB, Kitanidis PK, Street RL. 2006. The Flow Convergence-Routing Hypothesis for Pool-Riffle Maintenance in Alluvial Rivers. *Water Resources Research* **42**(W10427, doi:10.1029/2005WR004391.).

Maddock I, Harby A, Wood PJ. 2013. Ecohydraulics: An Integrated Approach. John Wiley & Sons, Ltd. Chichester, UK.

Marks K, Bates P. 2000. Integration of high-resolution topographic data with floodplain flow models. *Hydrological Processes* **14** : 2109–2122.

Moir HJ and Pasternack GB. 2008. Relationships between mesoscale morphological units, stream hydraulics and Chinook salmon (Oncorhynchus tshawytscha) spawning habitat on the Lower Yuba River. California, *Geomorphology* **100(3-4)** : 527-548.

Mouton AM, Schneider M, Depestele J, Goethals PLM, De Pauw N. 2007. Fish habitat modelling as a tool for river management. *Ecol. Eng* **29(3)** : 305-315.

Papanicolaou AN, Elhakeem Md, Dermisis D, Young N. 2011. Evaluation of the Missouri River shallow water habitat using a 2D-hydrodynamic model. *River Research and Applications* **27** : 157-167. doi: 10.1002/rra.1344

Pasternack GB. 2011. 2D Modeling and Ecohydraulic Analysis. Createspace: Seattle, WA.

Pasternack GB and Brown RA. 2013. Ecohydraulic Design of Riffle-Pool Relief and Morphological-Unit Geometry in Support of Regulated Gravel-Bed River Rehabilitation. (Maddock, I., Harby, A., Kemp, P., Wood, P., Eds.), Ecohydraulics: an integrated approach. John Wiley & Sons, Ltd. Chichester, UK.

Pasternack GB and Senter AE. 2011. 21st Century instream flow assessment framework for mountain streams. California Energy Commission, PIER. CEC-500-2013-059.

Pasternack GB, Bounrisavong MK, Parikh KK. 2008. Backwater control on riffle-pool hydraulics, fish habitat quality, and sediment transport regime in gravel-bed rivers. *Journal of Hydrology* **357** :1-2:125-139.

Pasternack GB, Fulton AA, Morford SL. 2010. Yuba River analysis aims to aid spring-run Chinook salmon habitat rehabilitation. *California Agriculture* **64** : 2 : 69-77.

Pasternack GB, Gilbert A, Wheaton J, Buckland E. 2006. Error propagation for velocity and shear stress prediction using 2D models for environmental management. *Journal of Hydrology* **328** : 227-241.

Pasternack GB, Tu D, Wyrick JR. 2014. Chinook adult spawning physical habitat of the lower Yuba River. Prepared for the Yuba Accord River Management Team. University of California, Davis, CA, 154pp.

Pasternack GB, Wang CL, Merz J. 2004. Application of a 2D hydrodynamic model to reach-scale spawning gravel replenishment on the lower Mokelumne River, California. *River Research and Applications* **20** :2:205-225.

Payne TR and Bremm DJ. 2003. The influence of multiple velocity calibration sets on the PHABSIM habitat index. Paper presented to International IFIM User's Workshop, June 1-5, 2003, Ft. Collins, CO.

Payne TR, Eggers SD, Parkinson DB. 2004. The number of transects required to compute a robust PHABSIM habitat index. *Hydroécologie Appliquée* **14(1)** : 27-53.

Prestininzi P, Di Baldassarre G, Schumann G, Bates PD. 2011. Selecting the appropriate hydraulic model structure using low-resolution satellite imagery. *Advances in Water Resources* **34(1)** : 38-46.

Railsback SF, Harvey BC, Sheppard C. 2012. InSTREAM: the individual-based stream trout research and environmental assessment model – Version 5.0. Model description. Lang, Railsback & Associates, Arcata, California. 101 p.

Sawyer AM, Pasternack GB, Moir HJ, Fulton AA. 2010. Riffle-Pool Maintenance and Flow Convergence Routing Confirmed on a Large Gravel Bed River. *Geomorphology* **114** :143-160.

Shelley J and Gibson S. 2015. Modeling Bed Degredation and In-Channel Mining in a Large Sand-Bed river with HEC-RAS 5.0. 10th Federal Interagency Sediment Conference, Reno, NV.

Snowling SD and Kramer JR. 2001. Evaluating modeling uncertainty for model selection. *Ecological Modeling* **138** : 17-30.

Stockdale RJ, McLelland SJ, Middleton R, Coulthard TJ. 2007. Measuring river velocities using GPS River Flow Tracers (GRiFTers). Wiley InterScience, *Earth Surface Processes and Landforms* **33** : 1315-1322.

Tayefi V, Lane SN, Hardy RJ, Yu D. 2007. A comparison of one- and two-dimensional approaches to modeling flood inundation over complex upland floodplains. *Hydrological Processes* **21(23)** : 3190-3202.

USACE. 2009. HEC-GeoRAS GIS Tools for Support of HEC-RAS using ArcGIS, Hydrologic Engineering Center, Davis, CA, 246 pp..

USACE. 2010. HEC-RAS River analysis System, Hydraulic Reference Manual, Version 4.1, Hydrologic Engineering Center, Davis, CA, 417 p.

Waddle T, Steffler P, Ghanem A, Katopodis C, Locke A. 2000. Comparison of One and Two-Dimensional Open Channel Flow Models for a Small Habitat Stream. *Rivers* **7(3)** : 205-220.

Weber, L.J., Goodwin, R.A., Li., S., Nestler, J.M., Anderson, J.J. 2006. Application of an Eulerian–Lagrangian–Agent method (ELAM) to rank alternative designs of a juvenile fish passage facility. Journal of Hydroinformatics 8:4:271–295.

Werner, M.G.F. 2004. A comparison of flood extent modeling approaches through constraining uncertainties on gauge data. Hydrology and Earth System Sciences 8(6), 1141-1152.

White, J. Q., Pasternack, G. B., and Moir, H. J. 2010. Valley width variation influences riffle-pool location and persistence on a rapidly incising gravel-bed river. Geomorphology 121:206-221.

Wu, R.S., Mao, C.T. 2007. The assessment of river ecology and habitat using a two-dimensional hydrodynamic and habitat model. Journal of Marine Science and Technology 15(4): 322-330.

Wyrick, J.R., and Pasternack, G.B. 2012. Landforms of the Lower Yuba River. Prepared for the Yuba Accord River Management Team. University of California at Davis, Davis, CA, 91pp.

Wyrick, J.R., and Pasternack, G.B. 2014. Geospatial organization of fluvial landforms in a gravel-cobble river: beyond the riffle-pool couplet. Geomorphology 213: 48-65. doi:10.1016/j.geomorph.2013.12.040.

Yuba Accord River Management Team. 2013. Aquatic Resources of the Lower Yuba River Past, Present & Future: Yuba Accord Monitoring and Evaluation Program Draft Interim Report.

Table 1: Research questions, hypotheses and test metrics.

Question	Hypothesis	Metric and Test Applied to Evaluate
Question 1: How well does a 1D model replicate 2D depth results?	1D depth residuals will be relatively small but will increase upstream (e.g. channelize residuals < meandering residuals < anastomosing residuals).	1. Computed depth residuals between each cell of the 1D and 2D depth grids and the evaluate residual distributions, summarizing them with a 'median absolute residual depth' statistic. 2. Plot 1D depths against 2D depths (scatter plot) and evaluate the performance of the 1D model based on the R^2 of the relationship.
Question 2: How well does a conveyance distributed 1D model replicate 2D velocity results?	1D velocity residuals will be much larger than the depth residuals and will also increase upstream.	Compare 1D and 2D velocity results with the same metrics and analyses as the depth residuals (from Question 1): 1. Median absolute velocity residual. 2. Scatter plot, slope, R^2.
Question 3: What Hydraulic processes generate large 1D residuals?	1D results will diverge from the 2D results in regions where lateral velocities are significant (e.g. flow separation, flow shadows, backwaters).	Map residuals to identify regions of high residual, and associate the hydraulic process connected to these regions.

Table 2: Morphological metrics and classifications of the three reaches.

	Reach 1	Reach 2	Reach 3
Entrenchment Ratio ($2XQ_{max}$)*	2.2	1.7	0.8
Entrenchment Ratio ($2XD_{max}$)*	4.6	1.7	1.0
Width/Depth Ratio	23	73	41
Sinuosity	1.18	1.07	1.19
Slope	0.00058	0.0017	0.0022
Gradation (d_{mean})	9-107 mm	47-116 mm	61-179 mm
Rosgen Classification	C3c	C3/4	D3

*computed for a water surface profile twice the max flow
**computed for a water surface profile twice the max depth

Table 3: Flow-roughness factors used to calibrate 1D Reaches.

Flow	Reach 1	Reach 2	Reach 3
Base Flow (28 cms)	1.1	1	1.2
Bank Full (142 cms)	0.99	0.95	1.1
Flood Flow (497 cms)	1.03	1	1.06

Table 4: Average calibration residuals and standard deviation of residuals (cm) after application of flow roughness factors.

Flow	Reach 1 Average/SD	Reach 2 Average/SD	Reach 3 Average/SD
Base Flow (28 cms)	-0.2/6.0	-2.7/8.1	-0.7/10.8
Bank Full (142 cms)	-0.5/4.4	-0.3/4.0	-1.5/7.8
Flood Flow (497 cms)	-1.0/3.6	-1.3/5.2	-1.5/8.4

Table 5: Median relative depth residuals for the three reaches and three flows modeled.

	Reach 1	Reach 2	Reach 3
	Confined	Meander	Anastomosing
Base Flow	3.9%	6.4%	7.2%
Bank Full	2.0%	3.6%	5.4%
Flood Flow	0.5%	2.6%	4.0%

.

Table 6: Median relative velocity residuals for the three reaches and three flows modeled.

	Reach 1	Reach 2	Reach 3
	Confined	Meander	Anastomosing
Base Flow	12.9%	13.0%	18.1%
Bank Full	9.6%	12.7%	14.6%
Flood Flow	10.2%	22.4%	16.2%

Table 7: Coefficient of Determination and Median Absolute Residuals for Reach 3, for all three flows, with the single reach and split flow modeling approaches.

	Depth		Velocity	
	Reach 3 Single Reach	Reach 3 Split Flow	Reach 3 Single Reach	Reach 3 Split Flow
	R^2 / $\lvert\tilde{\varepsilon}\rvert$	R^2 / $\lvert\tilde{\varepsilon}\rvert$	R^2 / $\lvert\tilde{\varepsilon}\rvert$	R^2 / $\lvert\tilde{\varepsilon}\rvert$
Base Flow	0.89/7.2%	0.96/6.9%	0.52/18.1%	0.70/16.6%
Bank Full	0.96/5.4%	0.97/4.3%	0.69/14.6%	0.77/12.5%
Flood Flow	0.98/4.0%	0.98 /3.8%	0.81/16.2%	0.84/17.3%

Figure 1: Map of the lower Yuba River with the three modeling reaches.

Figure 2: HEC-RAS geometries for split flow and single reach models for Reach 3.

Figure 3: Cross section velocity plot from HEC-RAS, where laterally distributed velocities are computed from the section average velocity with conveyance principles. HEC-RAS computed a composite cross section weighted velocity of 2.0 m/s for this cross section and a composite channel velocity of 2.4 m/s.

Figure 4: Scatter plot depth results and coefficient of determination for paired 1D and 2D depth results from each grid cell.

Figure 5: Scatter plot velocity results and coefficient of determination for paired 1D and 2D velocity results from each grid cellFigure 6: Velocity residuals for the three flows in Reach 1.

Figure 7: Velocity residuals for the three flows in Reach 2.

Figure 8: Velocity residuals for the three flows in Reach 3.

Figure 9: Depth and velocity residuals for the flood flow in Reach 2 with high residual zones annotated.

Figure 10: Zone of maximum velocity residual with 2:1 expansion rule of thumb for ineffective flow areas.

Figure 11: 1D velocity map, 2D velocity map and velocity residual map of the classical bar geometry in Reach 1.

Figure 12: Schematic of errors introduced at flows higher and lower than the design flow for 1D, split flow, modeling.

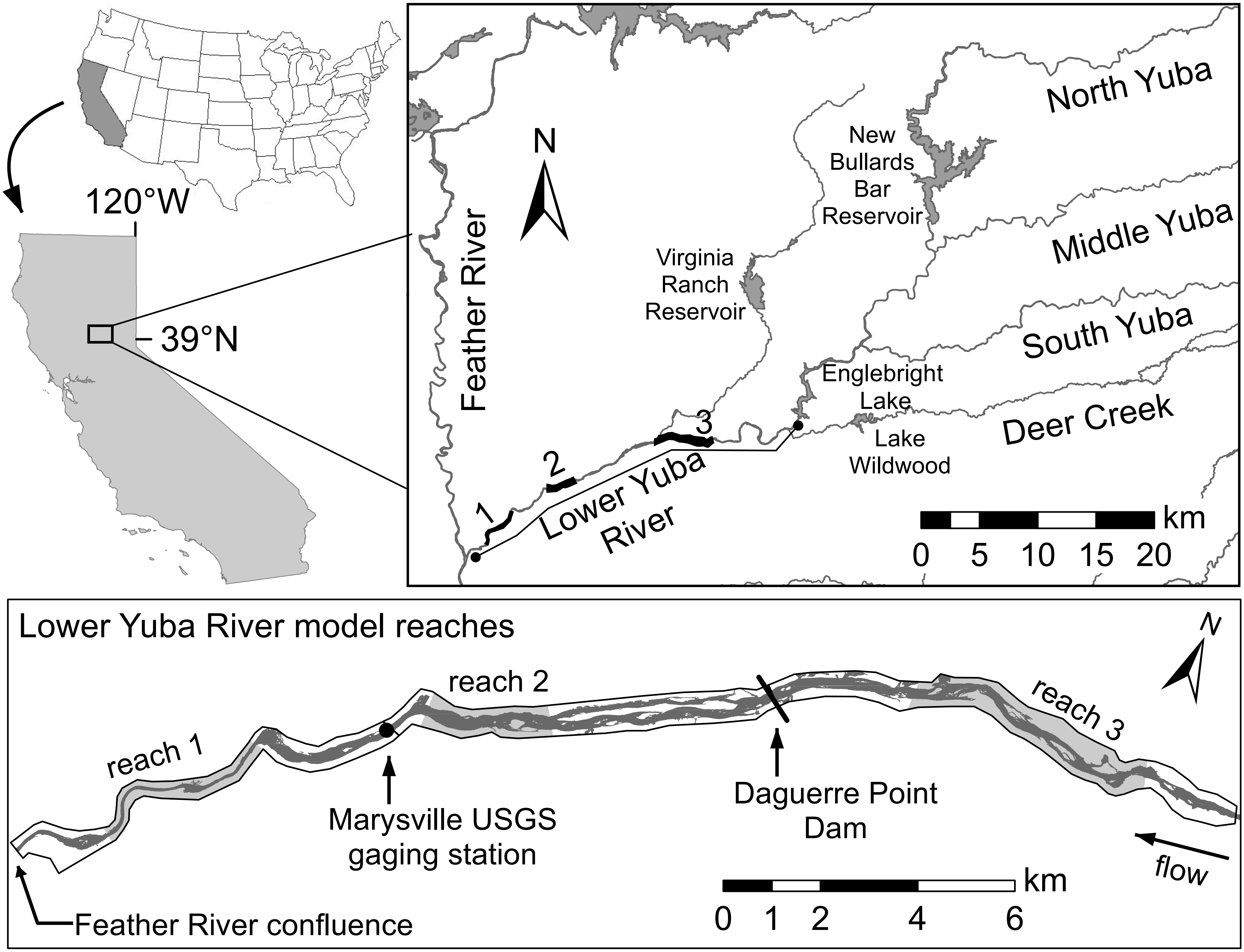

120°W
39°N
N
North Yuba
New
Bullards
Bar
Reservoir
Middle Yuba
Virginia
Ranch
Reservoir
South Yuba
Feather River
Englebright
Lake
Deer Creek
3
2
1
Lake
Wildwood
Lower Yuba
River
km
0 5 10 15 20
Lower Yuba River model reaches
N
reach 2
reach 1
reach 3
Marysville USGS
gaging station
Daguerre Point
Dam
flow
km
0 1 2 4 6
Feather River confluence

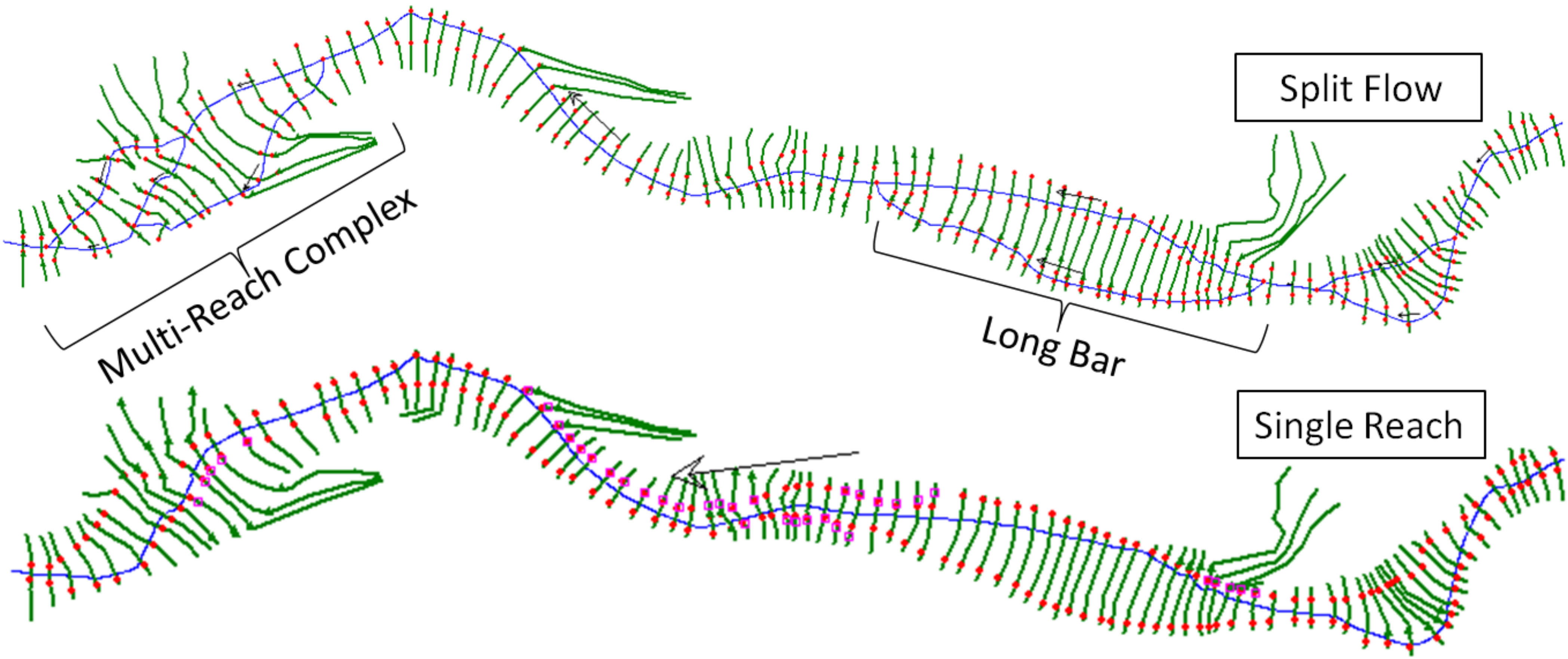
Split Flow
Long Bar
Multi-Reach Complex
Single Reach

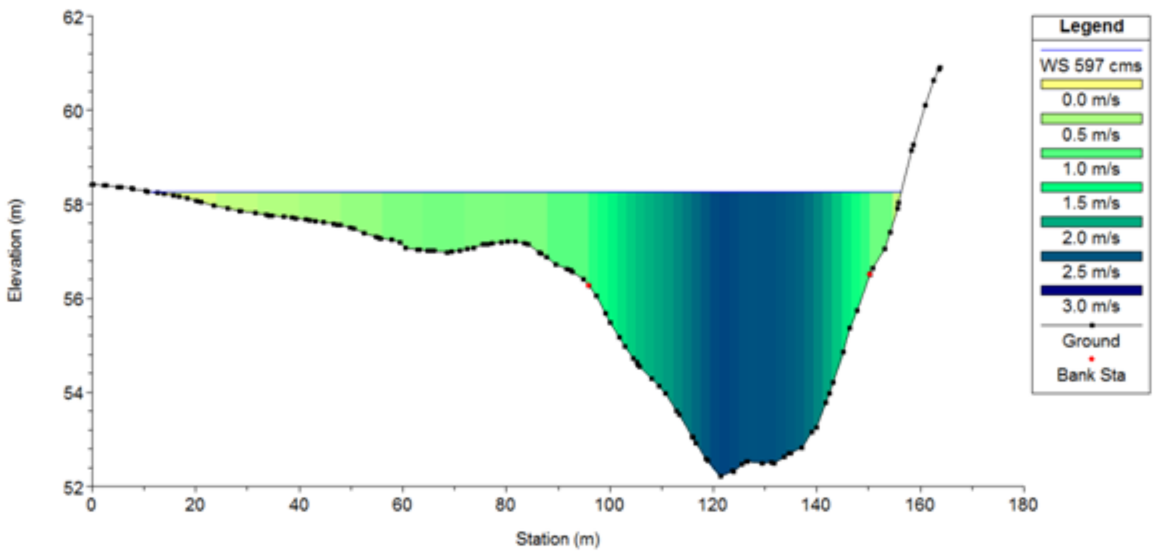

Legend
WS 597 cms
0.0 m/s
0.5 m/s
1.0 m/s
1.5 m/s
2.0 m/s
2.5 m/s
3.0 m/s
Ground
Bank Sta
Elevation (m)
Station (m)
62
60
58
56
54
52
0
20
40
60
80
100
120
140
160
180

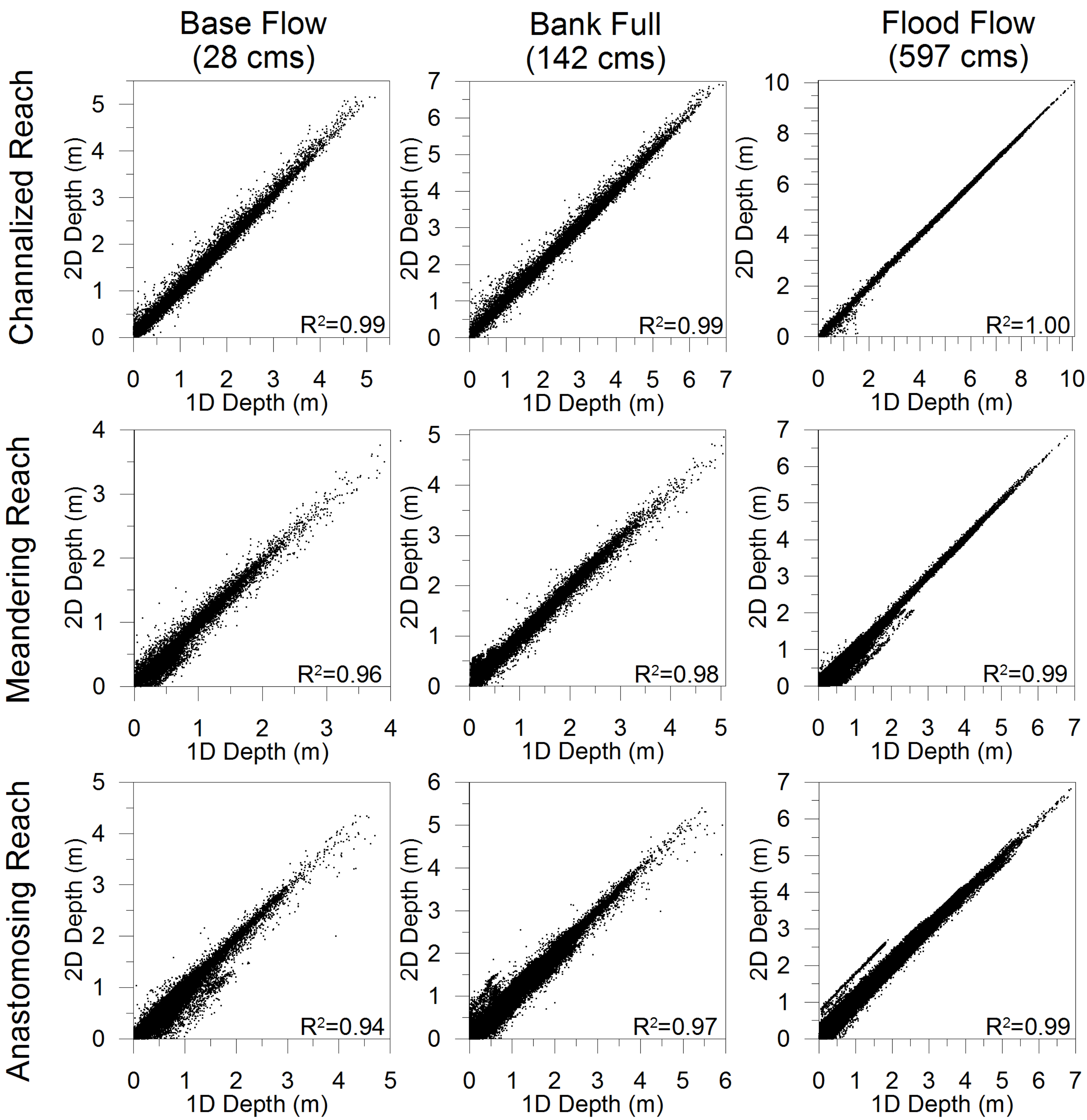

Base Flow
(28 cms)
Bank Full
(142 cms)
Flood Flow
(597 cms)
Channalized Reach
Meandering Reach
Anastomosing Reach
2D Depth (m)
1D Depth (m)
R²=0.99
R²=0.99
R²=1.00
R²=0.96
R²=0.98
R²=0.99
R²=0.94
R²=0.97
R²=0.99

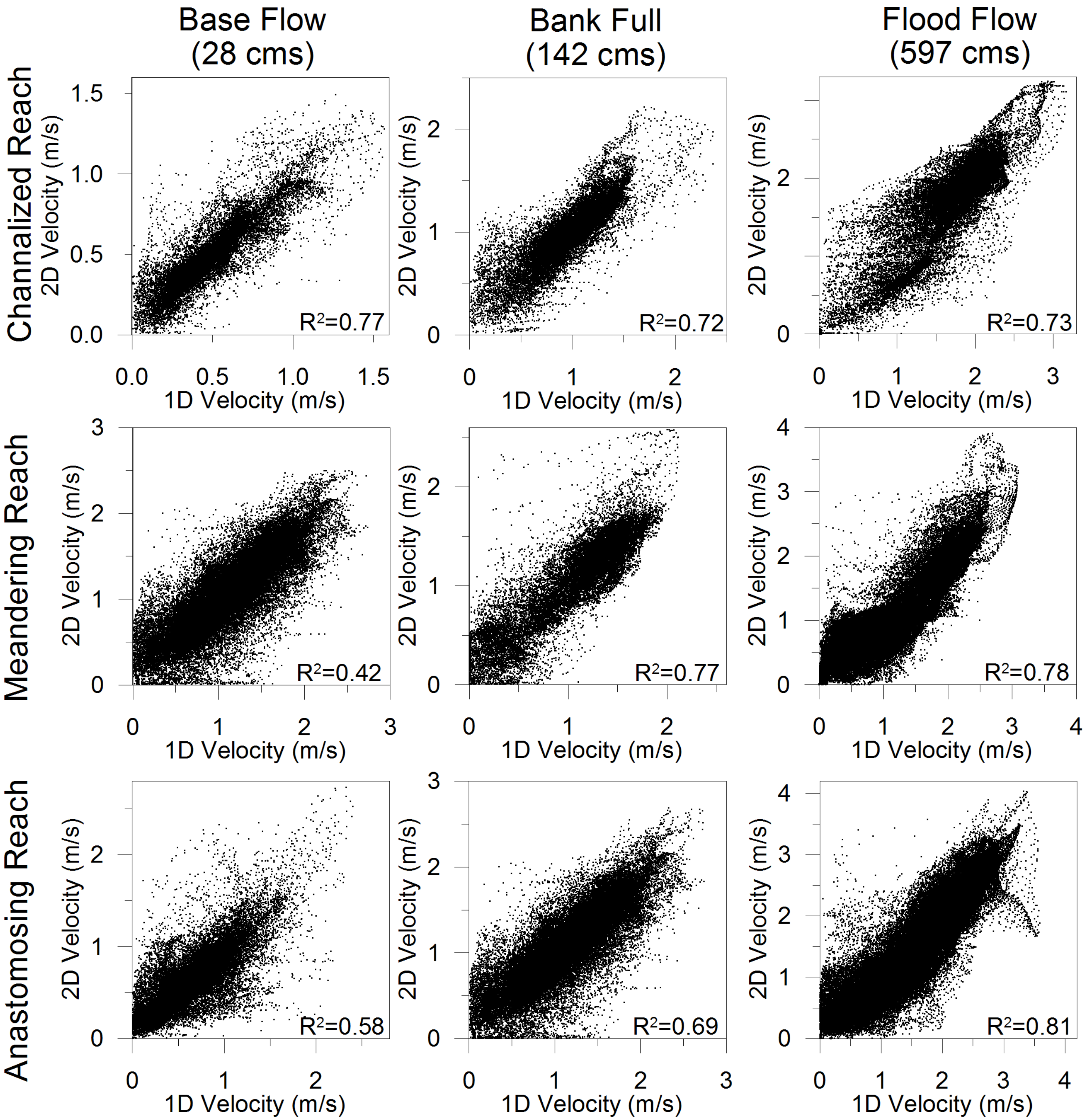
Base Flow (28 cms)
Bank Full (142 cms)
Flood Flow (597 cms)
Channalized Reach
Meandering Reach
Anastomosing Reach
2D Velocity (m/s)
1D Velocity (m/s)
R²=0.77
R²=0.72
R²=0.73
R²=0.42
R²=0.77
R²=0.78
R²=0.58
R²=0.69
R²=0.81

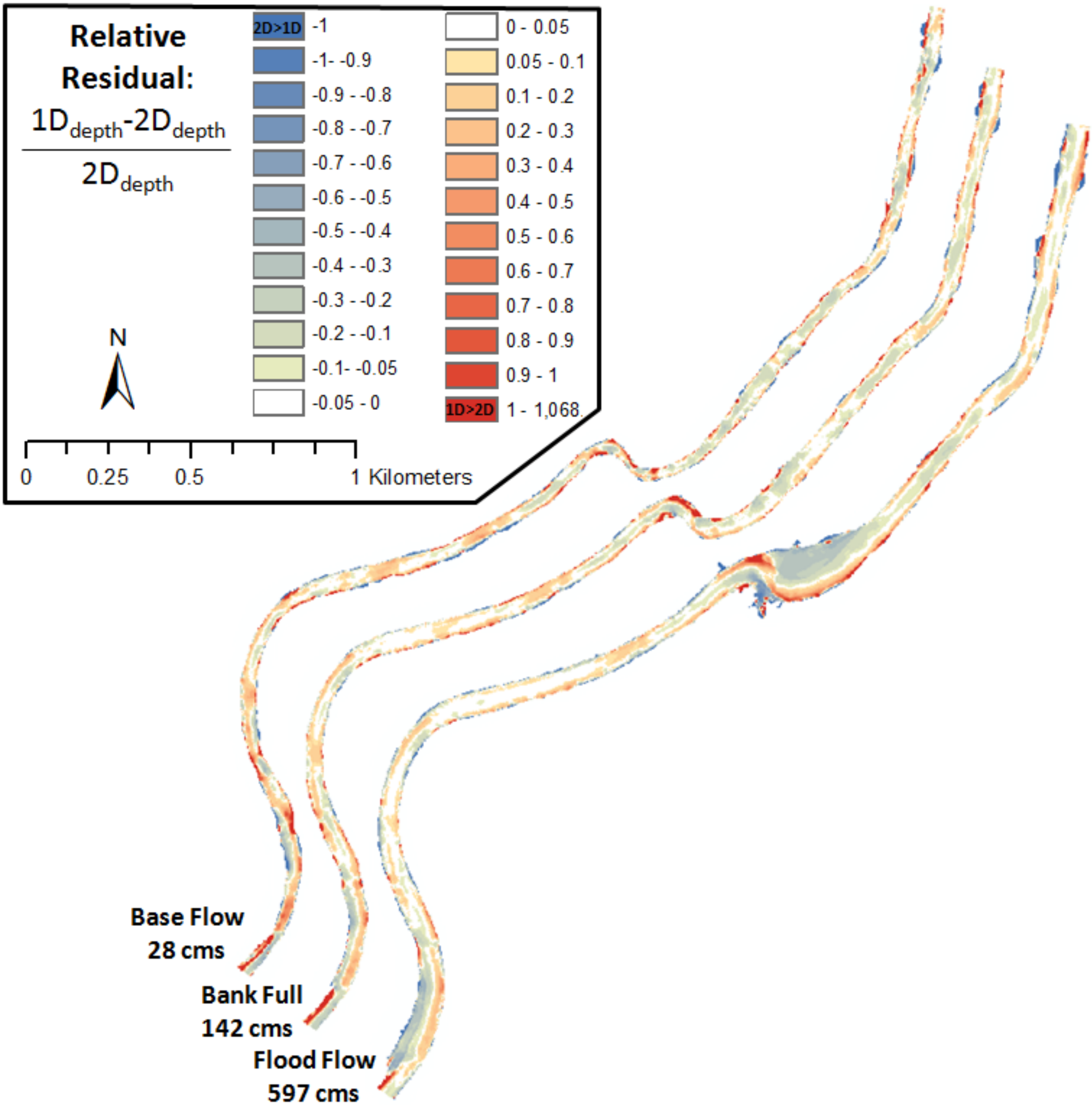

Relative Residual:
$\frac{1D_{depth}-2D_{depth}}{2D_{depth}}$
2D>1D -1
-1- -0.9
-0.9 - -0.8
-0.8 - -0.7
-0.7 - -0.6
-0.6 - -0.5
-0.5 - -0.4
-0.4 - -0.3
-0.3 - -0.2
-0.2 - -0.1
-0.1- -0.05
-0.05 - 0
0 - 0.05
0.05 - 0.1
0.1 - 0.2
0.2 - 0.3
0.3 - 0.4
0.4 - 0.5
0.5 - 0.6
0.6 - 0.7
0.7 - 0.8
0.8 - 0.9
0.9 - 1
1D>2D 1 - 1,068
N
0 0.25 0.5 1 Kilometers
Base Flow
28 cms
Bank Full
142 cms
Flood Flow
597 cms

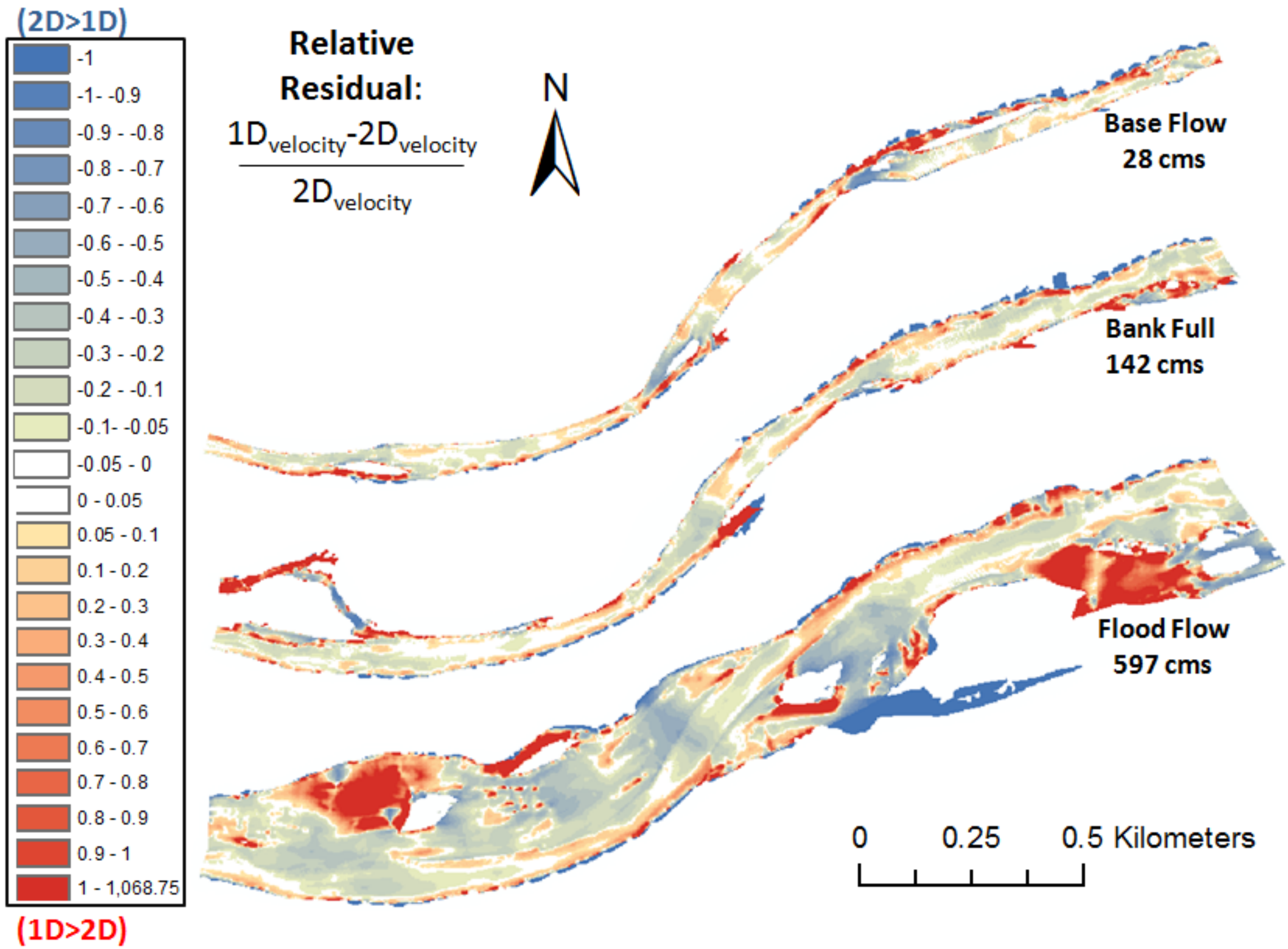
(2D>1D)
-1
-1- -0.9
-0.9 - -0.8
-0.8 - -0.7
-0.7 - -0.6
-0.6 - -0.5
-0.5 - -0.4
-0.4 - -0.3
-0.3 - -0.2
-0.2 - -0.1
-0.1- -0.05
-0.05 - 0
0 - 0.05
0.05 - 0.1
0.1 - 0.2
0.2 - 0.3
0.3 - 0.4
0.4 - 0.5
0.5 - 0.6
0.6 - 0.7
0.7 - 0.8
0.8 - 0.9
0.9 - 1
1 - 1,068.75
(1D>2D)
Relative
Residual:
$\frac{1D_{velocity}-2D_{velocity}}{2D_{velocity}}$
N
Base Flow
28 cms
Bank Full
142 cms
Flood Flow
597 cms
0
0.25
0.5 Kilometers

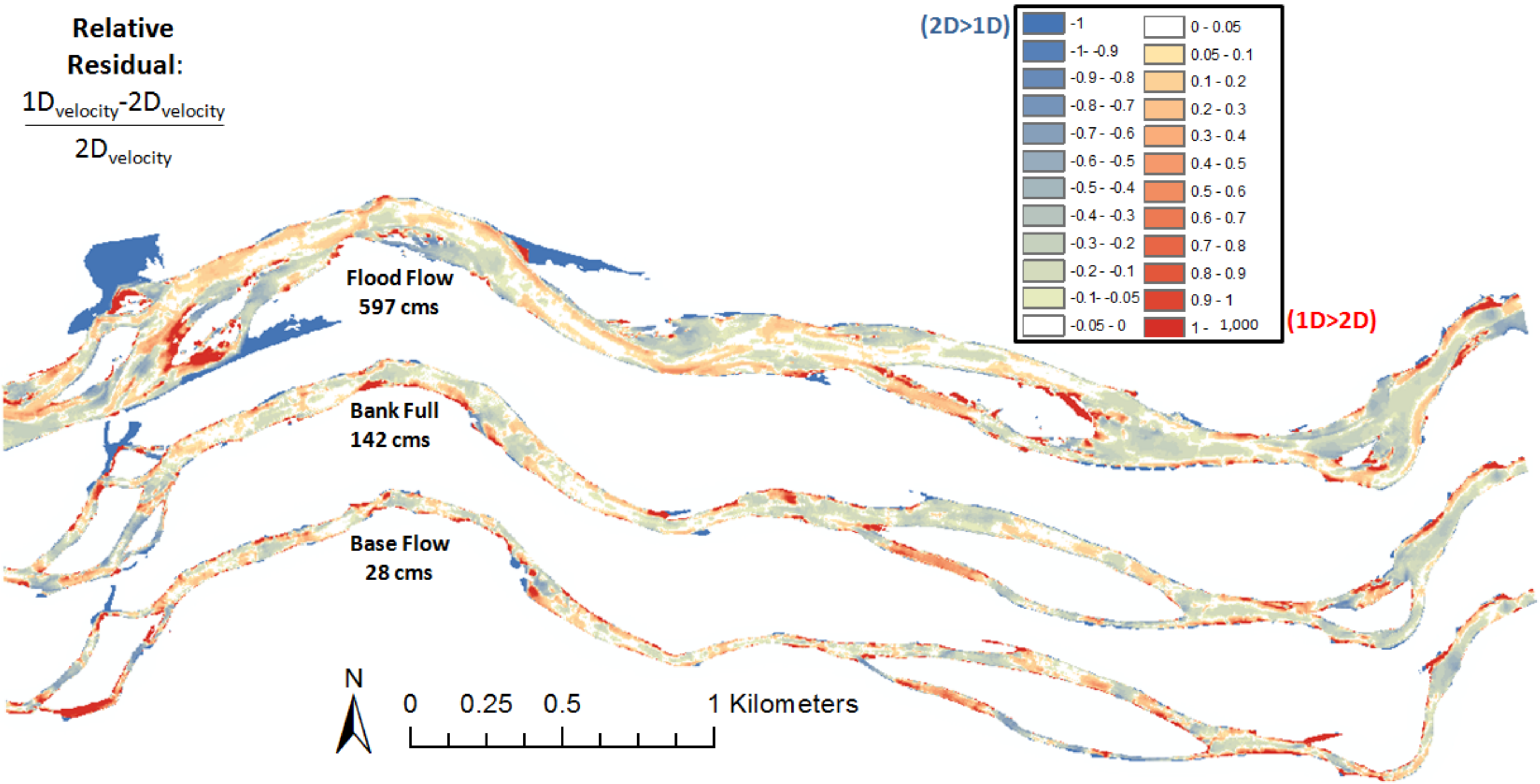
Relative Residual:
$\frac{1D_{velocity}-2D_{velocity}}{2D_{velocity}}$
(2D>1D)
-1
-1- -0.9
-0.9 - -0.8
-0.8 - -0.7
-0.7 - -0.6
-0.6 - -0.5
-0.5 - -0.4
-0.4 - -0.3
-0.3 - -0.2
-0.2 - -0.1
-0.1- -0.05
-0.05 - 0
0 - 0.05
0.05 - 0.1
0.1 - 0.2
0.2 - 0.3
0.3 - 0.4
0.4 - 0.5
0.5 - 0.6
0.6 - 0.7
0.7 - 0.8
0.8 - 0.9
0.9 - 1
1 - 1,000
(1D>2D)
Flood Flow
597 cms
Bank Full
142 cms
Base Flow
28 cms
N
0 0.25 0.5 1 Kilometers

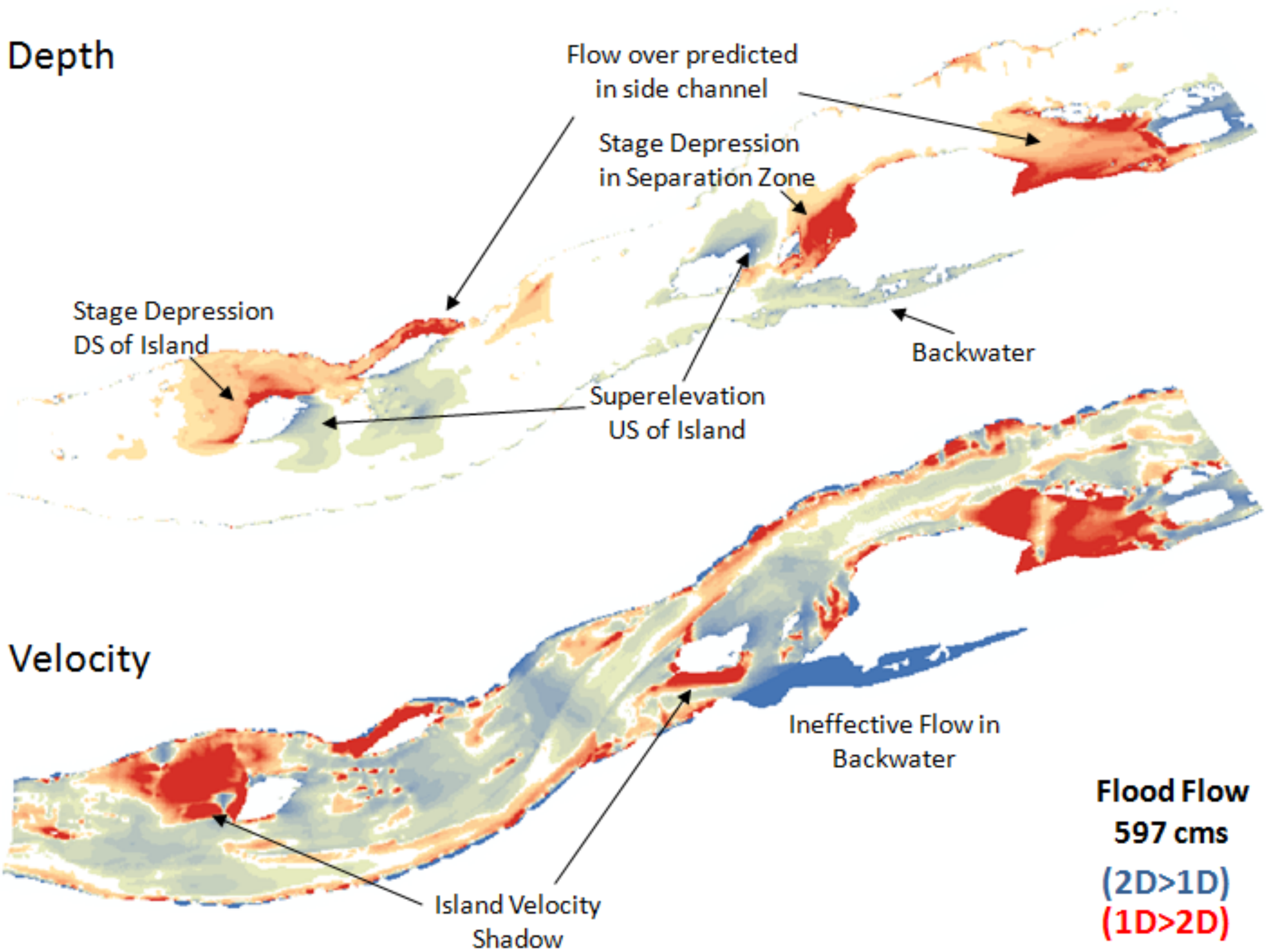
Depth
Flow over predicted in side channel
Stage Depression in Separation Zone
Stage Depression DS of Island
Backwater
Superelevation US of Island
Velocity
Ineffective Flow in Backwater
Flood Flow
597 cms
(2D>1D)
(1D>2D)
Island Velocity Shadow

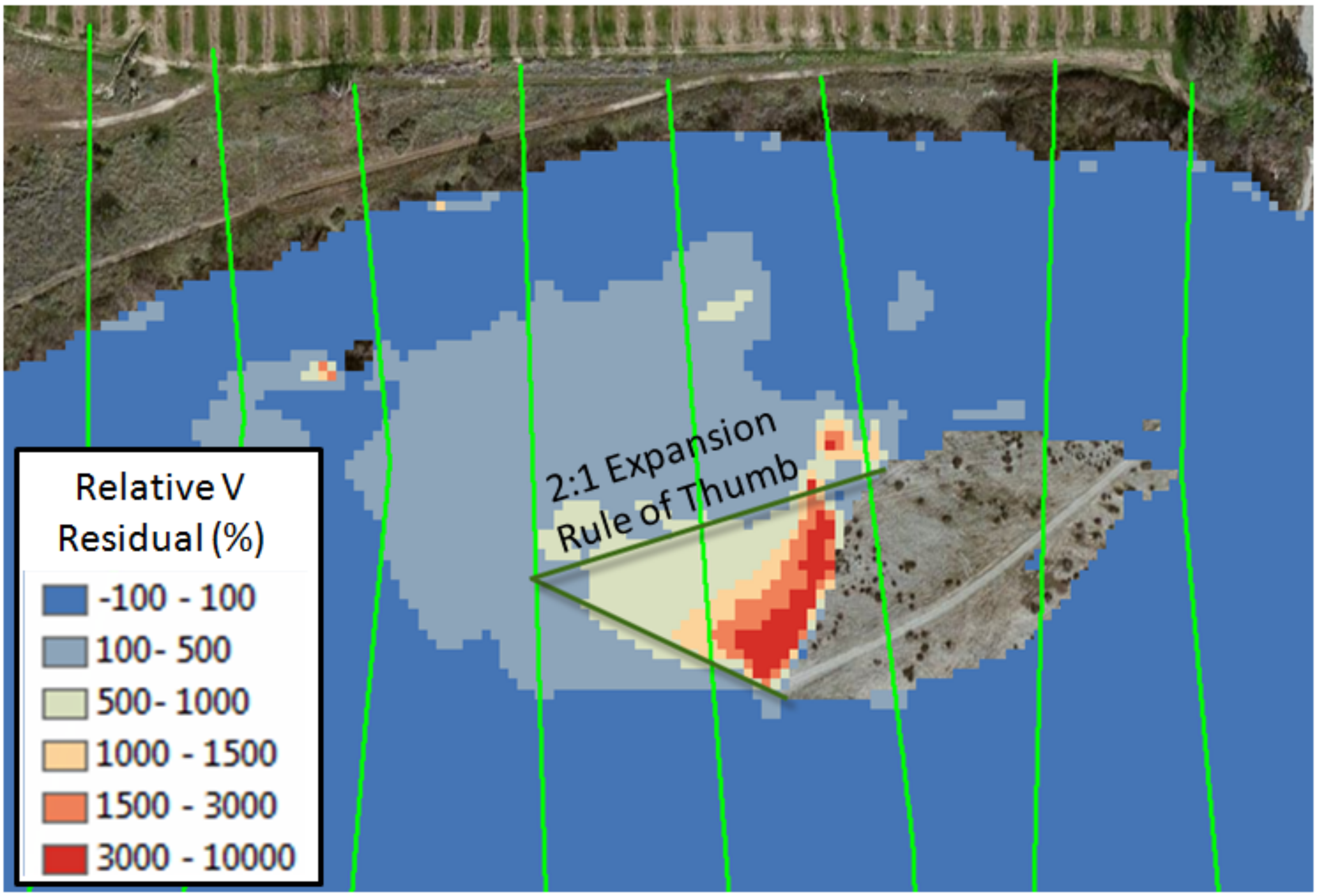
2:1 Expansion
Rule of Thumb
Relative V
Residual (%)
-100 - 100
100- 500
500- 1000
1000 - 1500
1500 - 3000
3000 - 10000

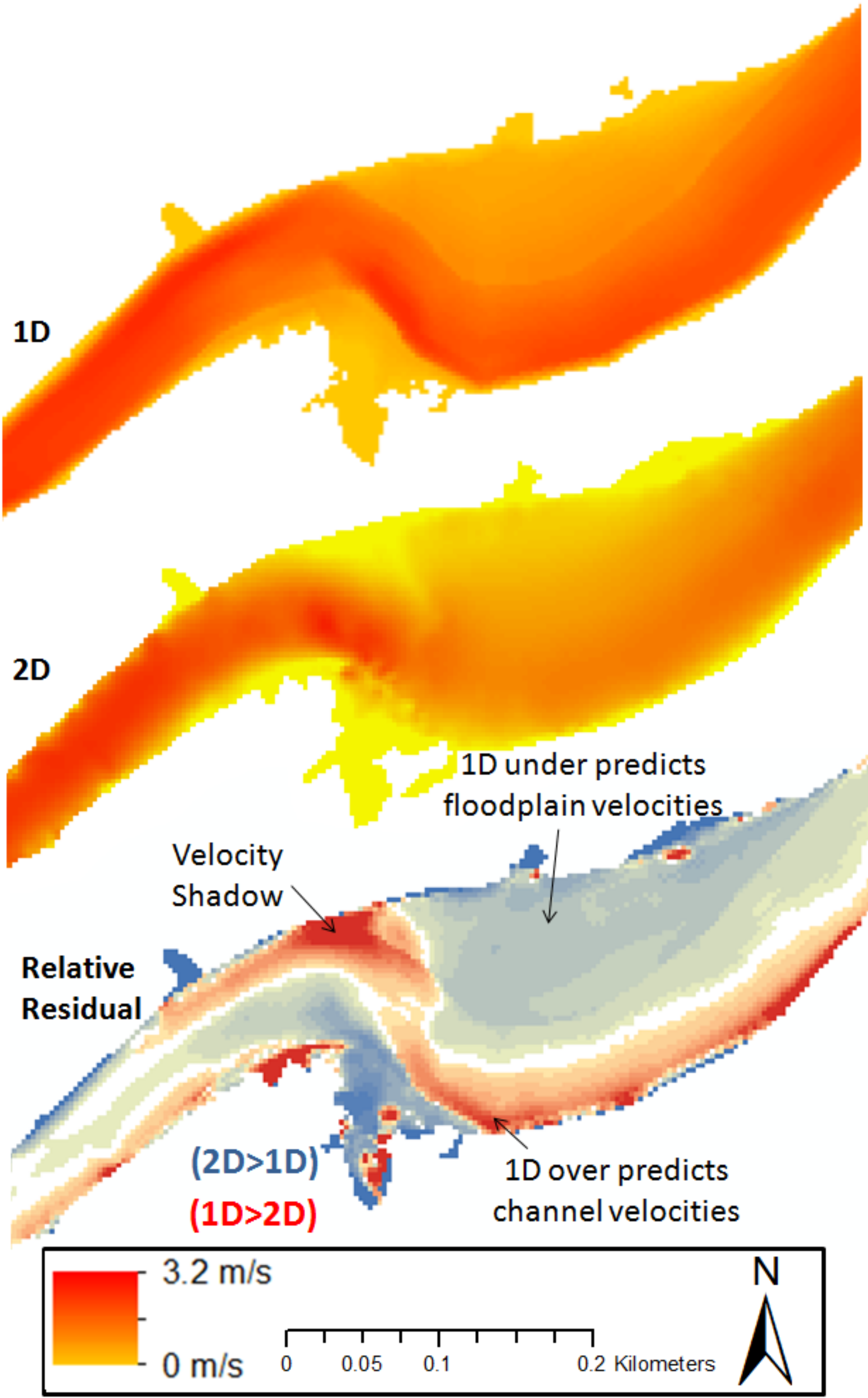

1D
2D
1D under predicts
floodplain velocities
Velocity
Shadow
Relative
Residual
(2D>1D)
(1D>2D)
1D over predicts
channel velocities
3.2 m/s
0 m/s
0
0.05
0.1
0.2 Kilometers
N

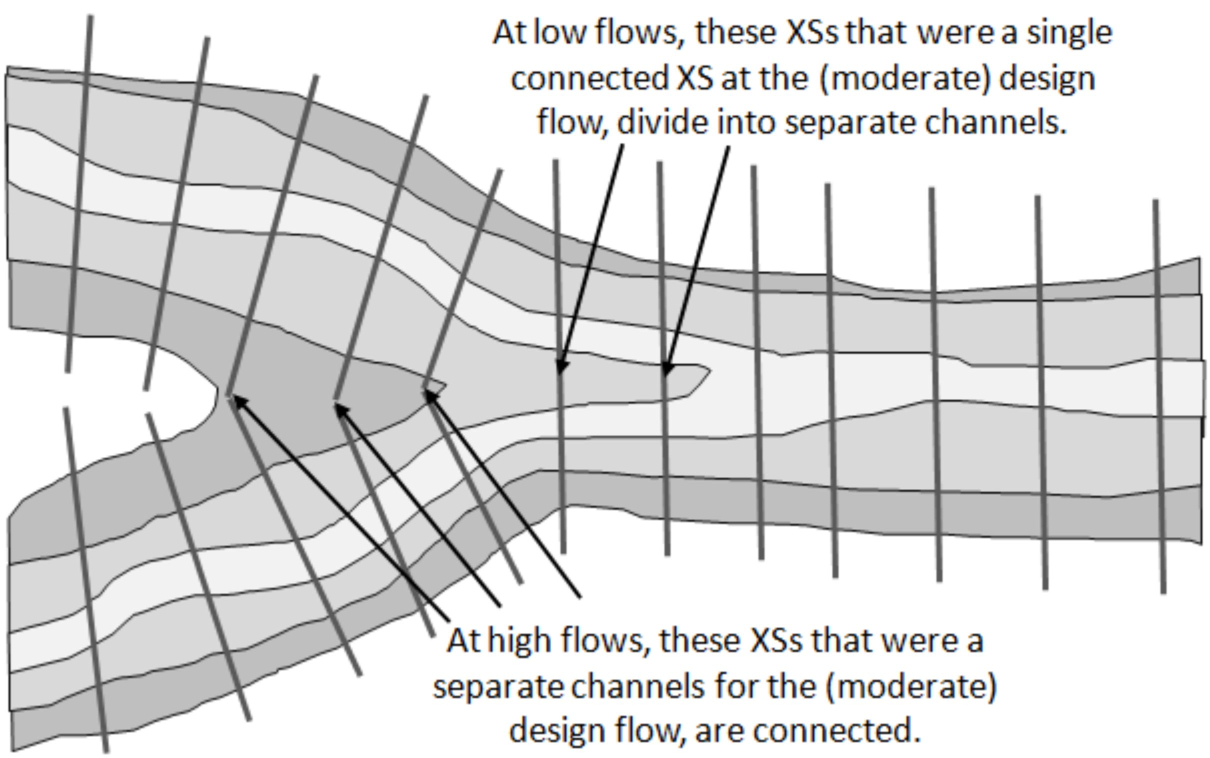
At low flows, these XSs that were a single connected XS at the (moderate) design flow, divide into separate channels.
At high flows, these XSs that were a separate channels for the (moderate) design flow, are connected.